EUROPEAN JOURNAL OF PURE AND APPLIED MATHEMATICS
2026, Vol. 19, Issue 1, Article Number 6805
ISSN 1307-5543 – ejpam.com
Published by New York Business Global

Exact Solutions and Stability Thresholds for the Fractional Gardner Equation with High-Order Dispersion

Wafaa B. Rabie[1], Hadeel Bin Amer[2], Hasib Khan[3,4,*], Jehad Alzabut[3,5], Dalia I. Elimy[6]

[1] *Department of Mathematics, Faculty of Science, Luxor University, Taiba, Luxor, Egypt*
[2] *Department of Computer Science, College of Computer and Information Sciences, Majmaah University, Al-Majmaah 11952, Saudi Arabia*
[3] *Department of Mathematics and Sciences, Prince Sultan University, 11586 Riyadh, Saudi Arabia*
[4] *Department of Mathematics, Shaheed Benazir Bhutto University, Sheringal, Dir Upper 18000, Khyber Pakhtunkhwa, Pakistan*
[5] *Department of Industrial Engineering, OSTIM Technical University, 06374 Ankara, Türkiye*
[6] *Department of Basic Science, Higher Institute of Engineering and Technology, Tanta, Egypt*

Abstract. This study investigates the fractional Gardner equation with high-order dispersion, a fundamental model for nonlinear wave propagation in plasmas, optical fibers, and fluid systems. Using the modified extended direct algebraic (mEDA) method, we derive exact analytical solutions including bright/dark solitons, singular waves, and periodic patterns. All solutions have been verified numerically using Mathematica to ensure their validity, as process innovation. The analysis reveals that the fractional order β significantly influences wave decay rates and memory effects, while specific parameter constraints govern solution existence and stability. A comprehensive linear stability analysis examines the modulation instability of the obtained solutions, revealing distinct regimes of marginal stability, instability, and stability based on dispersion relation characteristics. Physically, these solutions model wave phenomena in nonlinear optics, Bose–Einstein condensates, and oceanic systems, with the fractional order β providing crucial insights into non-local and memory-dependent processes. The stability analysis provides essential insights for practical wave manipulation applications. The combined analytical and stability approaches offer significant value for understanding nonlinear wave dynamics across various physical contexts.

2020 Mathematics Subject Classifications: 35C07, 35C08, 35C09
Key Words and Phrases: Fractional Gardner equation, higher-order dispersion effects, modified extended direct algebraic method, multi-waveform solutions, fractional parameter analysis, dynamical stability of nonlinear media.

*Corresponding author.
DOI: https://doi.org/10.29020/nybg.ejpam.v19i1.6805

Email addresses: wbr_allah_raby@yahoo.com (W. B. Rabie), h.binamer@mu.edu.sa (H. Bin Amer), hkhan@psu.edu.sa (H. Khan), jalzabut@psu.edu.sa (J. Alzabut), dalia.elimy@newinti.edu.my (D. I. Elimy)

1. Introduction

Over the past two decades, nonlinear partial differential equations (PDEs) with fractional derivatives have emerged as a transformative framework in applied mathematical research. This advancement has fundamentally reshaped our ability to model and analyze complex phenomena across diverse fields such as physics and engineering [1]. Unlike classical integer-order PDEs that are rooted in traditional calculus [2], fractional-order differential equations incorporate nonlocal operators—such as the Riemann-Liouville, Caputo, or Atangana-Baleanu fractional derivatives. These operators inherently capture memory effects, anomalous diffusion, and long-range spatial interactions, providing a superior tool for systems with power-law dynamics and hereditary properties [3]. The application of fractional calculus has proven indispensable in scenarios where conventional models fall short. For instance, in fluid dynamics, fractional derivatives naturally model the memory-dependent stress-strain relationships in viscoelastic fluids, a task at which classical Navier-Stokes equations struggle [4]. Similarly, in electrodynamics and plasma physics, accurate modeling of wave propagation in dispersive media with high-energy anomalies, such as superdiffusion in turbulent plasmas, demands the use of fractional calculus to derive correct dispersion relations [5]. Biological systems also benefit greatly from this approach; phenomena like neuron signal transmission or tumor growth often exhibit subdiffusive transport that cannot be replicated by integer-order PDEs without ad hoc modifications [6]. The theoretical foundations of fractional calculus have been significantly advanced through various mathematical frameworks. Karaca and Baleanu [7] explored evolutionary mathematical science and fractional modeling in complex systems, while Raza [8] provided comprehensive mathematical approaches to nonlinear dynamics. Recent studies by Khan et al. [9] and Baber et al. [10] have demonstrated innovative techniques for soliton solutions and synchronized wave analysis. Samir et al. [11] developed advanced methods for constructing optical solitons, and Demir [12] introduced hybrid fractional-order models with deep learning integration.

Applications of fractional calculus span numerous disciplines. In materials science, Umadevi et al. [13] modeled poroviscoelastic biofluid dynamics, while Kadyirov et al. [14], Galimzyanova et al. [15], and Yang et al. [16] investigated rheological behavior and ultrasonic treatment effects in crude oils. Zhou et al. [17, 18] developed rheological models for polymer composites deformation using time-fractional derivatives. Shalchi [19] applied fractional calculus to particle transport in cosmic plasmas, and Banda [20] analyzed fluid flow networks using hyperbolic systems. In quantum mechanics and advanced materials, Luchko [21] and Al-Raeei [22] applied fractional Schrödinger equations to quantum systems, while Pramanik et al. [23] and Müller et al. [24] developed fractional viscoelastic models for polymeric materials. Chandel and Swami [25] reviewed transport models in porous media, and Zaman et al. [26] explored soliton propagation in optical fibers. Recent advances in fractional calculus have expanded into chaos theory and complex dynamical systems. Almutairi and Saber [27] investigated chaotic behavior in the Lorenz–Lü–Chen system using Caputo operators, while Ahmed et al. [28] developed analytical solutions for variable-order fractional Liu systems. The intersection of fractional calculus with fun-

damental physics is demonstrated by Amoretti et al. [29] in cold antihydrogen research. Further contributions include chaos control in Newton-Leipnik systems [30], Burke-Shaw systems [31], controlled chaos of fractal-fractional Newton-Leipnik systems [32], and numerical approximations for Caputo-Fabrizio operators [33, 34]. The critical need for innovative solution techniques for these complex fractional nonlinear PDEs is highlighted by a growing body of recent literature. For example, the generalized exponential rational function method was effectively used to obtain optical soliton solutions for a dual-mode time-fractional nonlinear Schrödinger equation [35]. Multiple-type wave solutions for nonlinear coupled time-fractional Schrödinger models have also been explored [36]. Furthermore, various powerful approaches have been employed to derive innovative soliton solutions for generalized KdV equations [37]. The dynamics of multicomponent solitary waves in Gross-Pitaevskii systems of fractional order have been investigated, underscoring the richness of behaviors in these models [38]. From a numerical perspective, finite difference schemes like the β-fractional approach have been developed to solve challenging equations such as the time-fractional FitzHugh–Nagumo equation [39]. The mathematical foundation for these advances has been strengthened by theoretical developments in fractional calculus itself, such as the generalization of the Caputo derivative with respect to another function [40]. Moreover, recent applications extend to complex multidimensional settings, as demonstrated by wave propagation analysis in fractional generalized (3+1)-dimensional equations using local M-derivatives [41]. Computational advances in fractional modeling include significant contributions from Khan et al. [42–44] in epidemiological modeling and ecosystem analysis, and Rabie et al. [45] in wave solutions for fractional Boussinesq-KP equations. Elsonbaty et al. [46] and Sağlam et al. [47] developed novel methodologies for solitary wave solutions, while Kaur et al. [48] investigated shock wave perturbations in Gardner equations. Despite these significant advances, the analytical and numerical treatment of nonlinear fractional PDEs remains a formidable challenge, continually necessitating the development of new methodologies to derive exact solutions, assess their stability, and interpret their multi-scale dynamics [46, 47]. This research directly addresses these challenges by focusing on the fractional Gardner's equation, a prototypical model for nonlinear wave interactions in dispersive media [48].

Our work integrates high-order dispersion effects and fractional time derivatives within this framework. By applying the modified exponential decay analysis (mEDA) method, we aim to bridge existing methodological gaps and advance the computational toolkit for analyzing complex waveform phenomena. This contribution is particularly relevant for cutting-edge applications ranging from the propagation of optical solitons in metamaterials to the prediction of rogue waves in oceanography. This work bridges this gap by proposing a modified extended direct algebraic (mEDA), specifically tailored to address such complex cases. For the first time, we apply this approach to the perturbed fractional Gardner's equation with high-order dispersion. Our study builds upon the foundational work of Khalil et al. [49] in fractional derivative definitions and leverages recent advances in analytical and computational methods. The specific form of the equation we investigate

is expressed as follows [48].

$$\frac{\partial^\beta \mathcal{Q}}{\partial t^\beta} + \left(\sigma_5\ \mathcal{Q}^2 + \sigma_1\ \mathcal{Q}\right)\ \mathcal{Q}_x + \sigma_4\ \frac{\partial^{2\beta}\mathcal{Q}_x}{\partial t^{2\beta}} + \sigma_3\ \frac{\partial^\beta \mathcal{Q}_{\rm xx}}{\partial t^\beta} + \sigma_2\ \mathcal{Q}_{\rm xxx} - (\mathfrak{T}\ \mathcal{Q}^m\ \mathcal{Q}_x + \mathcal{V}\ \mathcal{Q}\ \mathcal{Q}_x \times \mathcal{Q}_{\rm xx} + \mathfrak{S}\ \mathcal{Q}_x \mathcal{Q}_{\rm xx} + \mathcal{J}\ \mathcal{Q}_x\ \mathcal{Q}_{\rm xxx} + \mathcal{A}\ \mathcal{Q}\ \mathcal{Q}_{\rm xxx} + \mathcal{U}\ \mathcal{Q}_{\rm xxxxx} + \mathcal{L}\ \mathcal{Q}\ \mathcal{Q}_{\rm xxxxx}) = 0, \tag{1}$$

where $\mathcal{Q}(x,t)$ represents the wave amplitude. The coefficients are defined as follows: σ_1 is the linear advection coefficient, σ_5 is the quadratic nonlinearity coefficient, σ_2, σ_3, and σ_4 represent the dispersion triplet (second, third, and fourth-order dispersion effects, respectively), $\mathfrak{T}$ is the power-law perturbation strength, $\mathcal{V}$ and $\mathfrak{S}$ are cross-nonlinearity coefficients, $\mathcal{J}$ and $\mathcal{A}$ are nonlinear dispersion coupling coefficients, and $\mathcal{U}$ and $\mathcal{L}$ represent fifth-order dispersion coefficients.

To ensure dimensional consistency in Eq. (1), we assign the following fundamental dimensions: length [L], time [T], and wave amplitude [A]. The fractional derivative operator $\partial^\beta/\partial t^\beta$ has dimensions $[\mathrm{T}]^{-\beta}$. Each term in Eq. (1) must have consistent dimensions of $[\mathrm{A}]\ [\mathrm{L}]^{-1}\ [\mathrm{T}]^{-\beta}$. The dimensional requirements for each coefficient are:

- σ_1: $[\mathrm{L}][\mathrm{T}]^{-\beta}[\mathrm{A}]^{-1}$
- σ_5: $[\mathrm{L}][\mathrm{T}]^{-\beta}[\mathrm{A}]^{-2}$
- σ_2, σ_3, σ_4: $[\mathrm{L}]^3[\mathrm{T}]^{-\beta}$, $[\mathrm{L}]^2$, $[\mathrm{L}][\mathrm{T}]^{\beta}$ respectively
- $\mathfrak{T}$: $[\mathrm{L}][\mathrm{T}]^{-\beta}[\mathrm{A}]^{-m}$
- $\mathcal{V}$, $\mathfrak{S}$: $[\mathrm{L}]^3[\mathrm{T}]^{-\beta}[\mathrm{A}]^{-2}$, $[\mathrm{L}]^3[\mathrm{T}]^{-\beta}[\mathrm{A}]^{-1}$
- $\mathcal{J}$, $\mathcal{A}$: $[\mathrm{L}]^4[\mathrm{T}]^{-\beta}[\mathrm{A}]^{-1}$, $[\mathrm{L}]^3[\mathrm{T}]^{-\beta}[\mathrm{A}]^{-1}$
- $\mathcal{U}$, $\mathcal{L}$: $[\mathrm{L}]^5[\mathrm{T}]^{-\beta}$, $[\mathrm{L}]^5[\mathrm{T}]^{-\beta}[\mathrm{A}]^{-1}$

This dimensional analysis confirms the mathematical consistency of our governing equation.

The β-fractional derivative of order $\beta \in (0,1]$, introduced by Khalil et al. [49], is defined as:

$$\frac{\partial^\beta \mathcal{Q}(x,t)}{\partial t^\beta} = \lim_{h\to 0} \frac{\mathcal{Q}\left(t + h\left(\frac{1}{\Gamma(\beta)} + t\right)^{1-\beta}\right) - \mathcal{Q}(t)}{h}, \quad \forall t > 0, \tag{2}$$

where $\Gamma(\cdot)$ is the Gamma function and β is the fractional order. This derivative operator satisfies the following fundamental properties:

(i) $\dfrac{\partial^\beta}{\partial t^\beta}\left(a\ \mathcal{Q}(t) + b\ \mathcal{R}(t)\right) = a\ \dfrac{\partial^\beta \mathcal{Q}(t)}{\partial t^\beta} + b\ \dfrac{\partial^\beta \mathcal{R}(t)}{\partial t^\beta}$ for any constants a and b.

(ii) $\dfrac{\partial^\beta}{\partial t^\beta}\left(\mathcal{Q}(t)\ \mathcal{R}(t)\right) = \mathcal{R}(t)\ \dfrac{\partial^\beta \mathcal{Q}(t)}{\partial t^\beta} + \mathcal{Q}(t)\ \dfrac{\partial^\beta \mathcal{R}(t)}{\partial t^\beta}$.

(iii) $\dfrac{\partial^\beta}{\partial t^\beta}\left(\dfrac{\mathcal{Q}(t)}{\mathcal{R}(t)}\right) = \dfrac{\mathcal{R}(t)\ \dfrac{\partial^\beta \mathcal{Q}(t)}{\partial t^\beta} - \mathcal{Q}(t)\ \dfrac{\partial^\beta \mathcal{R}(t)}{\partial t^\beta}}{(\mathcal{R}(t))^2}.$

(iv) $\dfrac{\partial^\beta}{\partial t^\beta}\left(\mathcal{Q}(\mathcal{R}(t))\right) = \dfrac{\partial^\beta \mathcal{Q}}{\partial \mathcal{R}}\dfrac{\partial^\beta \mathcal{R}}{\partial t^\beta}\mathcal{R}^{\beta-1}.$

(v) $\dfrac{\partial^\beta c}{\partial t^\beta} = 0,$ for any constant c.

For the special case when $\beta = 1$, the β-fractional derivative reduces to the classical derivative:

$$\left.\frac{\partial^\beta \mathcal{Q}(x,t)}{\partial t^\beta}\right|_{\beta=1} = \frac{\partial \mathcal{Q}(x,t)}{\partial t}. \tag{3}$$

While earlier studies [48] successfully derived shock and solitary wave solutions for the perturbed Gardner's equation using the G'/G-expansion method, their approach suffered from two fundamental limitations: restrictive parameter constraints that artificially narrowed the solution space and the inability to account for critical high-order dispersion effects. Our work introduces a transformative breakthrough through the modified extended direct algebraic method (mEDA) method, which delivers the first unified derivation of localized waves (bright/dark solitons, singular solitons), periodic structures (elliptic functions, periodic waves), and exotic solutions (hyperbolic, exponential forms). Furthermore, we establish comprehensive stability thresholds for these solutions through linear stability analysis, identifying precise conditions for marginal stability, instability, and asymptotic stability regimes. Our work builds upon foundational studies of the Gardner equation, particularly the recent investigation by Kaur et al. [48] which examined shock wave and singular solitary wave perturbations with dispersion triplet effects in the standard integer-order model.

The integration of exact solution derivation with stability analysis provides a complete framework for understanding nonlinear wave dynamics in fractional systems. This tripartite advancement not only subsumes previous results as special cases but establishes the first complete platform for investigating nonlinearity-dispersion-perturbation interactions in fractional Gardner systems, with demonstrated applications spanning from plasma wave dynamics to nonlinear optical signal processing. For other computational methods and statistical analysis, the readers can follow the results in [1, 42–44, 50, 51].

Systematic Research Framework: Section 2 introduces our innovative mEDA methodology. Section 3 presents new families of exact solutions obtained through this method and verified using advanced analytical techniques. Section 4 provides a comprehensive linear stability analysis, establishing stability thresholds for the obtained solutions. Section 5 discusses the physical interpretations of the extracted solutions. Section 6 synthesizes key breakthroughs and their implications for nonlinear wave theory, while Section 7 presents the main findings and discusses their significance in the broader context of nonlinear dynamical systems.

2. A Rigorous Analytical Foundations of the mEDA Technique

This section provides a rigorous mathematical formulation and implementation framework for the modified extended direct algebraic (mEDA), an advanced analytical technique designed to derive exact solutions for nonlinear partial differential equations (NPDEs). To demonstrate the method's efficacy, we employ the following general NPDE form as a model system [45]:

$$\mathcal{P}\left(\mathcal{Q}, \mathcal{Q}_x, \frac{\partial^\beta \mathcal{Q}}{\partial t^\beta}, \mathcal{Q}_{xx}, \dots\right) = 0. \tag{4}$$

Here, β-fractional derivative of order $\beta \in (0, 1]$, $\mathcal{P}$ represents a polynomial functional of the physical field $\mathcal{Q}(x, t)$ and its partial derivatives—both spatial (∂_x) and temporal (∂_t). This formulation encapsulates the essential nonlinear coupling structure and dynamical evolution of the system, encompassing a wide range of wave phenomena in mathematical physics.

Procedure-(1): We construct our analytical framework by proposing the following optimized ansatz for the wave solution:

$$\mathcal{Q}(x, t) = \mathcal{Y}(\mathcal{E}), \quad \mathcal{E} = x - \frac{\mathcal{G}}{\beta}\left(\frac{1}{\Gamma(\beta)} + t\right)^\beta, \tag{5}$$

where $\mathcal{G}$ is the wave velocity and $\mathcal{Y}(\mathcal{E})$ defines the wave profile's spatial structure. This change drastically simplifies the original PDE system to a nonlinear ordinary differential equation (ODE) framework by methodically applying the chain rule to convert derivatives as follows:

$$\mathcal{R}(\mathcal{Y},\ \mathcal{Y}',\ \mathcal{Y}'',\ \mathcal{Y}''',\ \dots) = 0. \tag{6}$$

Worked Example: Reduction to ODE Consider the fractional Gardner equation with high-order dispersion:

$$\frac{\partial^\beta \mathcal{Q}}{\partial t^\beta} + \alpha_1 \mathcal{Q}\mathcal{Q}_x + \alpha_2 \mathcal{Q}^2 \mathcal{Q}_x + \alpha_3 \mathcal{Q}_{xxx} + \alpha_4 \mathcal{Q}_{xxxxx} = 0. \tag{7}$$

Applying the ansatz (5) and using the chain rule for fractional derivatives, we obtain:

$$-\mathcal{G}\mathcal{Y}' + \alpha_1 \mathcal{Y}\mathcal{Y}' + \alpha_2 \mathcal{Y}^2 \mathcal{Y}' + \alpha_3 \mathcal{Y}''' + \alpha_4 \mathcal{Y}''''' = 0, \tag{8}$$

where primes denote derivatives with respect to $\mathcal{E}$. This demonstrates the systematic reduction from PDE to ODE.

Procedure-(2): Balance Principle Calculation: The balance principle determines the relationship between nonlinear and dispersion terms. Consider the highest-order derivative $\mathcal{Y}'''''$ and the strongest nonlinear term $\mathcal{Y}^2\mathcal{Y}'$:

$$\mathcal{Y}''''' \sim \mathcal{Y}^2 \mathcal{Y}'. \tag{9}$$

Assuming a solution of the form $\mathcal{Y} \sim \phi^m$, where ϕ satisfies an auxiliary equation, we equate the exponents:

$$m + 5 = 3m + 1 \quad \Rightarrow \quad 2m = 4 \quad \Rightarrow \quad m = 2. \tag{10}$$

This balance determines the appropriate solution form and ensures consistency in the algebraic elimination process. The complete algebraic elimination procedure involves substituting the solution ansatz into the ODE, applying the auxiliary equation constraints, and systematically solving the resulting algebraic system for the unknown coefficients.
Procedure-(3): To obtain exact analytical solutions to Eq. (4) via the proposed method, we express the solution as a finite series expansion of the form:

$$\mathcal{Y}(\mathcal{E}) = \sum_{j=-N}^{N} \ddot{a}_j \, \mathcal{R}(\mathcal{E})^j, \tag{11}$$

where $\ddot{a}_j$ be real-valued constant coefficients to be found, adhering to the non-degeneracy requirement $\ddot{a}_N^2 + \ddot{a}_{-N}^2 \neq 0$, which guarantees nontrivial answers.
Procedure-(4): To compute the balancing constant $\mathbb{N}$, we employ a rigorous approach based on the homogeneous balance principle (BP). This involves equating the scaling exponents of the dominant nonlinear term (e.g., $\mathcal{R}^p$) and the highest-order derivative (e.g., $\mathcal{R}^{(m)}$) in Eq. (6), The process yields the fundamental relation $N + m = pN$, which uniquely determines N, under specific conditions:

$$\mathcal{R}'(\mathcal{E}) = \epsilon\sqrt{\varrho_0 + \varrho_1 \, \mathcal{R}(\mathcal{E}) + \varrho_2 \;\; \mathcal{R}(\mathcal{E})^2 + \varrho_3 \, \mathcal{R}(\mathcal{E})^3 + \varrho_4 \, \mathcal{R}(\mathcal{E})^4 + \varrho_6 \, \mathcal{R}(\mathcal{E})^6}, \tag{12}$$

the parameter space of Eq. (12) is defined by the real coefficients ϱ_j $(j = 0, 1, 2, 3, 4)$ and the binary parameter $\epsilon \in \{-1, 1\}$. The complete solution space is obtained through systematic analysis of ϱ_j variations.
Procedure-(5):: Using different possible values for $\varrho_0, \varrho_1, \varrho_2, \varrho_3, \varrho_4, \varrho_6$, yields various types of solutions as follow:

Set(1): $\varrho_0 = \varrho_1 = \varrho_3 = \varrho_6 = 0$,

$$\mathcal{R}(\mathcal{E}) = \sqrt{-\frac{\varrho_2}{\varrho_4}}(\mathcal{E}\sqrt{\varrho_2}), \quad \varrho_2 > 0, \varrho_4 < 0.$$

$$\mathcal{R}(\mathcal{E}) = \sqrt{-\frac{\varrho_2}{\varrho_4}}\sec(\mathcal{E}\,\sqrt{-\varrho_2}), \quad \varrho_2 < 0, \varrho_4 > 0.$$

$$\mathcal{R}(\mathcal{E}) = \sqrt{-\frac{\varrho_2}{\varrho_4}}\csc(\mathcal{E}\,\sqrt{-\varrho_2}), \quad \varrho_2 < 0, \varrho_4 > 0.$$

Set(2): $\varrho_3 = \varrho_4 = \varrho_6 = 0$,

$$\mathcal{R}(\mathcal{E}) = \frac{\varrho_1 \sinh(2\mathcal{E}\sqrt{\varrho_2})}{2\varrho_2} - \frac{\varrho_1}{2\varrho_2}, \quad \varrho_2 > 0, \varrho_0 = 0.$$

$$\mathcal{R}(\mathcal{E}) = \frac{\varrho_1 \sin(\mathcal{E}\,\sqrt{-\varrho_2})}{2\varrho_2} - \frac{\varrho_1}{2\varrho_2}, \quad \varrho_2 < 0, \varrho_0 = 0.$$

$$\mathcal{R}(\mathcal{E}) = \sqrt{\frac{\varrho_0}{\varrho_2}}\sinh(\mathcal{E}\sqrt{\varrho_2}), \quad \varrho_0 > 0, \varrho_2 > 0, \varrho_1 = 0.$$

$$\mathcal{R}(\mathcal{E}) = \sqrt{-\frac{\varrho_0}{\varrho_2}}\sin(\mathcal{E}\ \sqrt{-\varrho_2}), \quad \varrho_0 > 0, \varrho_2 < 0, \varrho_1 = 0.$$

$$\mathcal{R}(\mathcal{E}) = exp(\mathcal{E}\sqrt{\varrho_2}) - \frac{\varrho_1}{2\varrho_2}, \quad \varrho_2 > 0, \varrho_0 = \frac{\varrho_1^2}{4\varrho_2}.$$

Set(3): $\varrho_0 = \varrho_1 = \varrho_2 = \varrho_6 = 0$,

$$\mathcal{R}(\mathcal{E}) = \frac{4\varrho_3}{\varrho_3^2\mathcal{E}^2 - 4\varrho_4}.$$

Set(4): $\varrho_0 = \varrho_1 = \varrho_6 = 0$,

$$\mathcal{R}(\mathcal{E}) = -\frac{\varrho_2\left(\tanh\left(\frac{\mathcal{E}\ \sqrt{\varrho_2}}{2}\right) + 1\right)}{\varrho_3}, \ \ \varrho_2 > 0.$$

$$\mathcal{R}(\mathcal{E}) = -\frac{\varrho_2\left(\coth\left(\frac{\mathcal{E}\ \sqrt{\varrho_2}}{2}\right) + 1\right)}{\varrho_3}, \ \ \varrho_2 > 0.$$

Set(5): $\varrho_0 = \varrho_1 = \varrho_6 = 0$,

$$\mathcal{R}(\mathcal{E}) = \frac{\varrho_2\text{sech}^2\left(\frac{\mathcal{E}\sqrt{\varrho_2}}{2}\right)}{2\sqrt{\varrho_2\varrho_4}\tanh\left(\frac{\mathcal{E}\sqrt{\varrho_2}}{2}\right) - \varrho_3}.$$

Set(6): $\varrho_1 = \varrho_3 = \varrho_6 = 0$,

No	ϱ_0	ϱ_2	ϱ_4	$\mathcal{R}(\mathcal{E})$
1	1	$-(1+m^2)$	m^2	$cd(\mathcal{E}, m)$ or $sn(\mathcal{E}, m)$
2	m^2	$-m^2+1$	1	$ns(\mathcal{E}, m)$ or $dc(\mathcal{E}, m)$
3	m^2-1	$2-m^2$	-1	$dn(\mathcal{E}, m)$
4	$\frac{m^2-1}{4}$	$\frac{m^2+1}{2}$	$\frac{m^2-1}{4}$	$m\ sd(\mathcal{E}, m) + nd(\mathcal{E}, m)$

Procedure-(6): Upon substituting Eqs. (11) and (12) into Eq. (6), we derive a polynomial in $\mathcal{R}$ of the form:

$$\sum_{j=-M}^{M} q_j\ \mathcal{R}^j(\zeta) = 0, \tag{13}$$

the coefficients q_j depend on the unknown constants ä$_j$ and the parameters ϱ_l, $(l = 0, 1, 2, 3, 4, 6)$ from Eq. (13). To satisfy the equation for all $\mathcal{R}$, we enforce the vanishing coefficient condition:

$$q_j = 0, \quad \forall j,$$

resulting in a nonlinear algebraic system for $\ddot{a}_j$ and ϱ_l, $(l = 0, 1, 2, 3, 4, 6)$. Employing symbolic computation, we solve this system to derive exact parameter constraints and obtain new families of soliton solutions for the governing equation.

2.1. Visual Overview of the mEDA Methodology

To enhance the clarity and pedagogical value of the modified extended direct algebraic (mEDA) technique, we present a comprehensive flowchart that systematically illustrates the step-by-step implementation procedure. This visual guide serves to elucidate the logical progression from the original nonlinear partial differential equation to the final exact solutions, highlighting the critical decision points and analytical transformations involved in the process. The flowchart effectively captures the method's structural elegance and provides researchers with an intuitive roadmap for applying the mEDA technique to various nonlinear physical models. The systematic approach demonstrated in this visualization underscores the method's robustness and computational efficiency in handling complex nonlinear phenomena across diverse scientific domains.

3. Complete Analytical Treatment of Perturbed Fractional Gardner's Equations

By implementing the traveling wave transformation (Eq. 5) with the critical parameter choice $m = 1$, the perturbed Gardner's equation (Eq. 1) collapses to a nonlinear ordinary differential equation (NLODE) of the form:

$$-(\mathcal{L}\,\mathcal{Y}+\mathcal{U})\,\mathcal{Y}^{(5)}+\left[-\mathcal{A}\,\mathcal{Y}+\left(\mathcal{G}^2\,\sigma_4-\mathcal{G}\,\sigma_3+\sigma_2\right)-\mathcal{J}\,\mathcal{Y}'\right]\mathcal{Y}^{(3)}-\mathcal{V}\mathcal{Y}\mathcal{Y}'\mathcal{Y}''+(\sigma_1-\mathfrak{T})\,\mathcal{Y}\,\mathcal{Y}'+$$
$$\sigma_5\mathcal{Y}^2\mathcal{Y}'-\mathfrak{S}\mathcal{Y}'\mathcal{Y}''-\mathcal{G}\mathcal{Y}'=0. \tag{14}$$

Leveraging the methodological framework from Section 2, we obtain a complete solution structure for Eq. (14) in the general form:

$$\mathcal{Y}=\ddot{a}_2\mathcal{R}(\mathcal{E})^2+\ddot{a}_1\mathcal{R}(\mathcal{E})+\ddot{a}_0+\frac{\ddot{a}_{-1}}{\mathcal{R}(\mathcal{E})}+\frac{\ddot{a}_{-2}}{\mathcal{R}(\mathcal{E})^2}, \tag{15}$$

where $\ddot{a}_j$ are real-valued coefficients subject to the non-degeneracy condition $\ddot{a}_2^2+\ddot{a}_{-2}^2\neq 0$. By inserting the ansatz (Eq. 15) into (Eq. 14) while enforcing the constraint (Eq. 12), and setting $a_0 = a_{-1} = a_1 = 0$, we obtain a polynomial in $\mathcal{R}(\mathcal{E})$. Equating coefficients of like powers to zero generates a system of nonlinear algebraic equations. We solve this system symbolically using Wolfram Mathematica, yielding the following solution classes:

First Case: When $\varrho_0 = \varrho_1 = \varrho_3 = \varrho_6 = 0$, the algebraic system yields a constrained solution set. This condition establishes a distinct mathematical framework that generates solutions with specific restrictions.

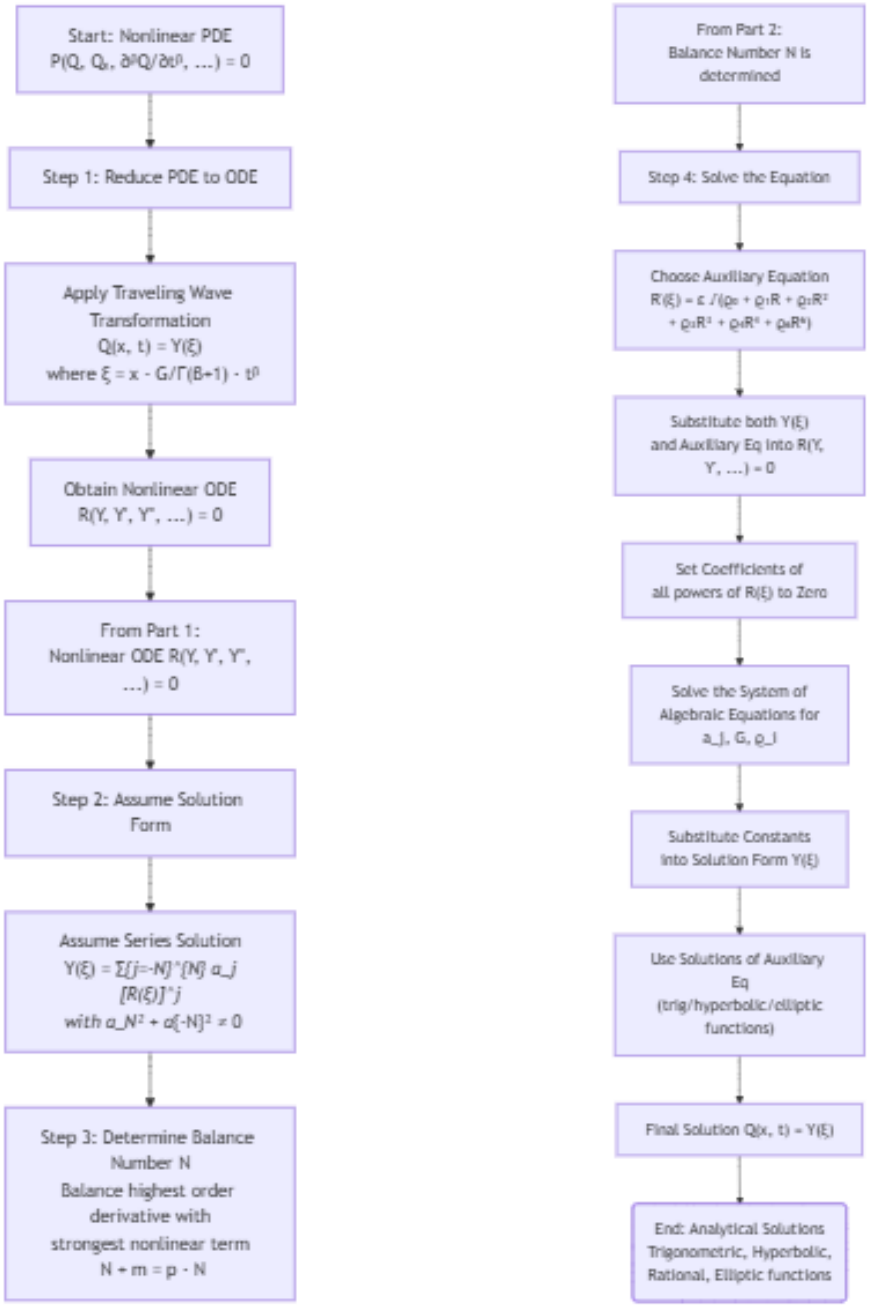

Figure 1: Flowchart illustrating the systematic procedure of the mEDA method for solving nonlinear partial differential equations.

$$\textbf{(1. 1)}\quad \ddot{a}_{-2}=0,\quad \ddot{a}_{2}=\frac{3\ \varrho_4\ (2\ \mathcal{A}+\mathfrak{S})\pm 3\sqrt{\varrho_4^2\ ((2\ \mathcal{A}+\mathfrak{S})^2+40\ \sigma_5\ \mathcal{U})}}{\sigma_5},\quad \sigma_4=\frac{\varrho_2(4\ \mathcal{G}\ \sigma_3-4\ \sigma_2+16\ \mathcal{U}\ \varrho_2)+\mathcal{G}}{4\ \mathcal{G}^2\ \varrho_2},$$

$$\sigma_1 = \frac{\varrho_4\ (\mathcal{G}(2\ \mathcal{A}+\mathfrak{S})+8\ \mathcal{U}\ \varrho_2\ (4\ \varrho_2\ (\mathcal{A}+20\ \mathcal{L}\ \varrho_2+3\ \mathfrak{S})+5\ \mathfrak{T}))\pm\left(\mathcal{G}-64\ \mathcal{U}\ \varrho_2^2\right)\sqrt{\varrho_4^2\ ((2\ \mathcal{A}+\mathfrak{S})^2+40\ \sigma_5\ \mathcal{U})}}{40\ \mathcal{U}\ \varrho_2\ \varrho_4},$$

$$\mathcal{V} = \frac{\mathcal{L}\ \left(\varrho_4\ (2\ \mathcal{A}+\mathfrak{S})\mp\sqrt{\varrho_4^2\ ((2\ \mathcal{A}+\mathfrak{S})^2+40\ \sigma_5\ \mathcal{U})}\right)}{2\ \mathcal{U}\varrho_4}, \quad \mathcal{J}=0.$$

(1. 2) $\ddot{a}_{-2} = \frac{2\ \varrho_2\ (\sigma_2-4\ \mathcal{U}\ \varrho_2)}{\mathfrak{S}\ \varrho_4},\ \ddot{a}_2 = \mathcal{G} = 0,\ \mathcal{V} = \frac{\sigma_5}{4\ \varrho_2},\ \mathcal{J}=0,\ \sigma_1 = 4\,\varrho_2\ (\mathcal{A}+4\ \mathcal{L}\ \varrho_2+\mathfrak{S})+\frac{\sigma_5(\sigma_2-4\ \mathcal{U}\ \varrho_2)}{\mathfrak{S}}+\mathfrak{T}.$

Based on the previously derived solution set(1.1), the solutions to (Eq. 1) emerge in the following general form:

(1.1. 1) When the following conditions are satisfied $\sigma_5\ \mathcal{U} > 0,\ \varrho_2 > 0,\ \sigma_5 \neq 0$, and $\varrho_4 < 0,$:

$$\mathcal{Q}_{1.1.1} = -\frac{\varrho_2}{\sigma_5\ \varrho_4}\left(3\varrho_4\ (2\mathcal{A}+\mathfrak{S}) \pm 3\sqrt{\varrho_4^2\left[(2\mathcal{A}+\mathfrak{S})^2+40\sigma_5\ \mathcal{U}\right]}\right) sech^2\left[(x-\frac{\mathcal{G}}{\beta}\ \left(\frac{1}{\Gamma(\beta)}+t\right)^{\beta})\ \sqrt{\varrho_2}\right]. \tag{16}$$

(1.1. 2) When the following conditions are satisfied $\sigma_5\ \mathcal{U} > 0,\ \varrho_2 < 0,\ \sigma_5 \neq 0$, and $\varrho_4 > 0,$ the singular periodic solutions can be expressed in the following form:

$$\mathcal{Q}_{1.1.2} = -\frac{\varrho_2}{\sigma_5\ \varrho_4}\left(3\varrho_4\ (2\mathcal{A}+\mathfrak{S}) \pm 3\sqrt{\varrho_4^2\left[(2\mathcal{A}+\mathfrak{S})^2+40\sigma_5\ \mathcal{U}\right]}\right) \sec^2\left[(x-\frac{\mathcal{G}}{\beta}\ \left(\frac{1}{\Gamma(\beta)}+t\right)^{\beta})\ \sqrt{-\varrho_2}\right], \tag{17}$$

and

$$\mathcal{Q}_{1.1.3} = -\frac{\varrho_2}{\sigma_5\ \varrho_4}\left(3\varrho_4\ (2\mathcal{A}+\mathfrak{S}) \pm 3\sqrt{\varrho_4^2\left[(2\mathcal{A}+\mathfrak{S})^2+40\sigma_5\ \mathcal{U}\right]}\right) \csc^2\left[(x-\frac{\mathcal{G}}{\beta}\ \left(\frac{1}{\Gamma(\beta)}+t\right)^{\beta})\ \sqrt{-\varrho_2}\right]. \tag{18}$$

Based on the previously derived solution set(1.2), the solutions to (Eq. 1) emerge in the following general form:

(1.2. 1) When the following conditions are satisfied $\varrho_2 > 0,\ \mathfrak{S} \neq 0$, and $\varrho_4 < 0,$ the hyperbolic solution can be expressed in the following form:

$$\mathcal{Q}_{1.2.1} = \frac{2\ (4\,\mathcal{U}\varrho_2-\sigma_2)}{\mathfrak{S}}\ \cosh^2\left[(x-\frac{\mathcal{G}}{\beta}\ \left(\frac{1}{\Gamma(\beta)}+t\right)^{\beta})\ \sqrt{\varrho_2}\right]. \tag{19}$$

(1.2. 2) When the following conditions are satisfied $\mathfrak{S} \neq 0,\ \varrho_2 < 0$, and $\varrho_4 > 0,$ the periodic solutions can be expressed in the following form:

$$\mathcal{Q}_{1.2.2} = \frac{2\ (4\,\mathcal{U}\ \varrho_2-\sigma_2)}{\mathfrak{S}}\ \cos^2\left[(x-\frac{\mathcal{G}}{\beta}\ \left(\frac{1}{\Gamma(\beta)}+t\right)^{\beta})\ \sqrt{-\varrho_2}\right], \tag{20}$$

and

$$\mathcal{Q}_{1.2.3} = \frac{2\ (4\,\mathcal{U}\ \varrho_2-\sigma_2)}{\mathfrak{S}}\ \sin^2\left[(x-\frac{\mathcal{G}}{\beta}\ \left(\frac{1}{\Gamma(\beta)}+t\right)^{\beta})\ \sqrt{-\varrho_2}\right]. \tag{21}$$

Second Case: When $\varrho_1 = \varrho_3 = \varrho_6 = 0$, the algebraic system yields a constrained solution set. This condition establishes a distinct mathematical framework that generates solutions with specific restrictions.

(2. 1) $\ddot{a}_{-2} = 0,\ \ddot{a}_2 = \frac{3\ \varrho_4\ (2\ \mathcal{A}+\mathfrak{S})\pm 3\ \sqrt{\varrho_4^2((2\ \mathcal{A}+\mathfrak{S})^2+40\ \sigma_5\ \mathcal{U})}}{\sigma_5},\ \mathcal{V} = \frac{\mathcal{L}\ \left(\varrho_4(2\ \mathcal{A}+\mathfrak{S})\mp\sqrt{\varrho_4^2\ ((2\ \mathcal{A}+\mathfrak{S})^2+40\ \sigma_5\ \mathcal{U})}\right)}{2\ \mathcal{U}\varrho_4},$

$\mathcal{J} = 0,\ \sigma_4 = \frac{1}{4\mathcal{G}^2\sigma_5\varrho_2}[6\varrho_0(\varrho_4(2\mathcal{A}\mathfrak{S}+12\sigma_5\mathcal{U}+\mathfrak{S}^2)\mp\mathfrak{S}\sqrt{\varrho_4^2((2\mathcal{A}+\mathfrak{S})^2+40\sigma_5\mathcal{U})})+$
$\sigma_5(4\varrho_2(\mathcal{G}\sigma_3-$

$\sigma_2+4\mathcal{U}\ \varrho_2)+\mathcal{G})],\ \sigma_1 = \frac{1}{40\ \mathcal{U}\ \varrho_2\ \varrho_4}24\mathcal{U}\ \varrho_0\ \varrho_4^2\ (6\ \mathcal{A}-80\ \mathcal{L}\ \varrho_2-7\ \mathfrak{S})\mp\frac{1}{40\ \mathcal{U}\ \varrho_2\ \varrho_4}\left(\mathcal{G}-64\ \mathcal{U}\ \varrho_2^2\right)$

$\times\sqrt{\varrho_4^2\ ((2\ \mathcal{A}+\mathfrak{S})^2+40\ \sigma_5\ \mathcal{U})}+\frac{1}{40\mathcal{U}\ \varrho_2\ \varrho_4}[\varrho_4(\mathcal{G}(2\mathcal{A}+\mathfrak{S})+8\mathcal{U}(9\varrho_0\sqrt{\varrho_4^2((2\mathcal{A}+\mathfrak{S})^2+40\sigma_5\mathcal{U})}+$

$4\varrho_2^2\ (\mathcal{A}+20\mathcal{L}\varrho_2+3\mathfrak{S})+5\mathfrak{T}\varrho_2))].$

(2. 2) $\ddot{a}_{-2} = \frac{3\left(\varrho_0(2\mathcal{A}+\mathfrak{S})\pm\sqrt{\varrho_0^2((2\mathcal{A}+\mathfrak{S})^2+40\sigma_5\ \mathcal{U})}\right)}{\sigma_5},\ \ddot{a}_2 = 0,\ \mathcal{V} = \frac{\mathcal{L}\left(\varrho_0(2\mathcal{A}+\mathfrak{S})\pm\sqrt{\varrho_0^2((2\ \mathcal{A}+\mathfrak{S})^2+40\ \sigma_5\mathcal{U})}\right)}{2\mathcal{U}\ \varrho_0},$

$\mathcal{J} = 0,\ \sigma_4 = \frac{1}{4\mathcal{G}^2\ \sigma_5\ \varrho_2}[\sigma_5\ (4\ \varrho_2\ (\mathcal{G}\ \sigma_3-\sigma_2+4\ \mathcal{U}\ \varrho_2)+\mathcal{G})+6\varrho_0\ \varrho_4\ (\mathfrak{S}(2\ \mathcal{A}+\mathfrak{S})+12\ \sigma_5\ \mathcal{U})$

$\mp 6\ \mathfrak{S}\ \varrho_4\ \sqrt{\varrho_0^2\ ((2\ \mathcal{A}+\mathfrak{S})^2+40\ \sigma_5\ \mathcal{U})}],\ \sigma_1 = \frac{1}{40\ \mathcal{U}\ \varrho_0\ \varrho_2}(24\,\mathcal{U}\ \varrho_0^2\ \varrho_4\ (6\ \mathcal{A}-80\ \mathcal{L}\ \varrho_2-7\ \mathfrak{S})$

$\mp\left(\mathcal{G}-64\ \mathcal{U}\ \varrho_2^2\right)\sqrt{\varrho_0^2\ ((2\ \mathcal{A}+\mathfrak{S})^2+40\ \sigma_5\ \mathcal{U})}\varrho_0\ (\mathcal{G}\ (2\ \mathcal{A}+\mathfrak{S})+4\ \varrho_2^2\ (\mathcal{A}+20\ \mathcal{L}\ \varrho_2+3\ \mathfrak{S})+$

$5\mathfrak{T}\varrho_2)+8\ \mathcal{U}(-9\ \varrho_4\ \sqrt{\varrho_0^2\ ((2\ \mathcal{A}+\mathfrak{S})^2+40\ \sigma_5\ \mathcal{U})})).$

Based on the previously derived solution set(2.1), the solutions to (Eq. 1) emerge in the following general form:

(2.1. 1) When the following conditions are satisfied $\varrho_0 = 1,\ \varrho_2 = -m^2-1,\ \varrho_4 = m^2,\ (2\ \mathcal{A}+\mathfrak{S})^2+40\ \sigma_5\ \mathcal{U} > 0 > 0,\ \ \sigma_5 \neq 0$, and $0 < m \leq 1$, the Jacobi elliptic function (JEF) solutions can be expressed in the following form:

$$\mathcal{Q}_{2.1.1} = \frac{3\ m^2}{\sigma_5}\ \left[\left(\mathfrak{S}\pm\sqrt{(2\mathcal{A}+\mathfrak{S})^2+40\sigma_5\mathcal{U}}\right)+2\mathcal{A}\right]\ sn^2\left[x-\frac{\mathcal{G}}{\beta}\ \left(\frac{1}{\Gamma(\beta)}+t\right)^{\beta}\right], \tag{22}$$

or

$$\mathcal{Q}_{2.1.2} = \frac{3\ m^2}{\sigma_5}\ \left[\left(\mathfrak{S}\pm\sqrt{(2\mathcal{A}+\mathfrak{S})^2+40\sigma_5\mathcal{U}}\right)+2\mathcal{A}\right]\ cd^2\left[x-\frac{\mathcal{G}}{\beta}\ \left(\frac{1}{\Gamma(\beta)}+t\right)^{\beta}\right]. \tag{23}$$

By setting $m = 1$ in Eq. 22, we derive the dark soliton solution as follows:

$$\mathcal{Q}_{2.1.1,1} = \frac{3}{\sigma_5}\left[\left(\mathfrak{S} \pm \sqrt{(2\mathcal{A}+\mathfrak{S})^2 + 40\sigma_5\mathcal{U}}\right) + 2\mathcal{A}\right]\tanh^2\left[x - \frac{\mathcal{G}}{\beta}\left(\frac{1}{\Gamma(\beta)} + t\right)^{\beta}\right]. \tag{24}$$

(2.1. 2) When the following conditions are satisfied $\varrho_0 = m^2 - 1$, $\varrho_2 = 2 - m^2$, $\varrho_4 = -1$, $(2\,\mathcal{A} + \mathfrak{S})^2 + 40\,\sigma_5\,\mathcal{U} > 0$, $\sigma_5 \neq 0$, and $0 \leq m \leq 1$, the JEF solution can be expressed in the following form:

$$\mathcal{Q}_{2.1.3} = \frac{3}{\sigma_5}\left[\left(-\mathfrak{S} \pm \sqrt{(2\mathcal{A}+\mathfrak{S})^2 + 40\sigma_5\mathcal{U}}\right) - 2\mathcal{A}\right]^{\,2}\left[x - \frac{\mathcal{G}}{\beta}\left(\frac{1}{\Gamma(\beta)} + t\right)^{\beta}\right]. \tag{25}$$

By setting $m = 1$ in Eq. 25, we derive the bright soliton solution as follows:

$$\mathcal{Q}_{2.1.3,1} = \frac{3}{\sigma_5}\left[\left(-\mathfrak{S} \pm \sqrt{(2\mathcal{A}+\mathfrak{S})^2 + 40\sigma_5\mathcal{U}}\right) - 2\mathcal{A}\right] sech^2\left[x - \frac{\mathcal{G}}{\beta}\left(\frac{1}{\Gamma(\beta)} + t\right)^{\beta}\right]. \tag{26}$$

(2.1. 3) When the following conditions are satisfied $\varrho_0 = -m^2$, $\varrho_2 = 2m^2 - 1$, $\varrho_4 = 1 - m^2$, $(2\,\mathcal{A} + \mathfrak{S})^2 + 40\,\sigma_5\,\mathcal{U} > 0$, $\sigma_5 \neq 0$, and $0 \leq m < 1$, the JEF solution can be expressed in the following form:

$$\mathcal{Q}_{2.1.4} = \frac{3\left(1-m^2\right)}{\sigma_5}\left[\left(\mathfrak{S} \pm \sqrt{(2\mathcal{A}+\mathfrak{S})^2 + 40\sigma_5\mathcal{U}}\right) + 2\mathcal{A}\right] nc^2\left[x - \frac{\mathcal{G}}{\beta}\left(\frac{1}{\Gamma(\beta)} + t\right)^{\beta}\right]. \tag{27}$$

By setting $m = 0$ in Eq. 27, we derive the singular periodic solution as follows:

$$\mathcal{Q}_{2.1.4,1} = \frac{3}{\sigma_5}\left[\left(\mathfrak{S} \pm \sqrt{(2\mathcal{A}+\mathfrak{S})^2 + 40\sigma_5\mathcal{U}}\right) + 2\mathcal{A}\right]\sec^2\left[x - \frac{\mathcal{G}}{\beta}\left(\frac{1}{\Gamma(\beta)} + t\right)^{\beta}\right]. \tag{28}$$

(2.1. 4) When the following conditions are satisfied $\varrho_0 = 1$, $\varrho_2 = 2 - 4m^2$, $\varrho_4 = 1$, $(2\,\mathcal{A} + \mathfrak{S})^2 + 40\,\sigma_5\,\mathcal{U} > 0$, $\sigma_5 \neq 0$, and $0 \leq m \leq 1$, the JEF solution can be expressed in the following form:

$$\mathcal{Q}_{2.1.5} = \frac{3}{\sigma_5}\left[\left(\mathfrak{S} \pm \sqrt{(2\mathcal{A}+\mathfrak{S})^2 + 40\sigma_5\mathcal{U}}\right) + 2\mathcal{A}\right]^{\,2}\left[x - \frac{\mathcal{G}}{\beta}\left(\frac{1}{\Gamma(\beta)} + t\right)^{\beta}\right]$$
$$\times nc^2\left[x - \frac{\mathcal{G}}{\beta}\left(\frac{1}{\Gamma(\beta)} + t\right)^{\beta}\right] sn^2\left[x - \frac{\mathcal{G}}{\beta}\left(\frac{1}{\Gamma(\beta)} + t\right)^{\beta}\right]. \tag{29}$$

By setting $m = 1$ or $m = 0$ in Eq. 29, we derive the dark soliton solution or the singular periodic solution in the following form:

$$\mathcal{Q}_{2.1.5,1} = \frac{3}{\sigma_5}\left[\left(\mathfrak{S} \pm \sqrt{(2\mathcal{A}+\mathfrak{S})^2 + 40\sigma_5\mathcal{U}}\right) + 2\mathcal{A}\right]\tanh^2\left[x - \frac{\mathcal{G}}{\beta}\left(\frac{1}{\Gamma(\beta)} + t\right)^{\beta}\right], \tag{30}$$

or

$$\mathcal{Q}_{2.1.5,2} = \frac{3}{\sigma_5}\left[\left(\mathfrak{S} \pm \sqrt{(2\mathcal{A}+\mathfrak{S})^2 + 40\sigma_5\mathcal{U}}\right) + 2\mathcal{A}\right]\tan^2\left[x - \frac{\mathcal{G}}{\beta}\left(\frac{1}{\Gamma(\beta)} + t\right)^{\beta}\right]. \tag{31}$$

(2.1. 5) When the following conditions are satisfied $\varrho_0 = m^4 - 2m^3 + m^2$, $\varrho_2 = -\frac{4}{m}$, $\varrho_4 = -m^2 + 6m - 1$, $(2\ \mathcal{A} + \mathfrak{S})^2 + 40\ \sigma_5\ \mathcal{U} > 0$, $\sigma_5 \neq 0$, and $0 < m \leq 1$, the JEF solution can be expressed in the following form:

$$\mathcal{Q}_{2.1.6} = \frac{3\ m^2[(m-6)\ m+1]\ \left[\left(-\mathfrak{S} \pm \sqrt{(2\ \mathcal{A}+\mathfrak{S})^2 + 40\ \sigma_5\ \mathcal{U}}\right) - 2\ \mathcal{A}\right]}{\sigma_5} \times \frac{cn^2\left[x - \frac{\mathcal{G}}{\beta}\left(\frac{1}{\Gamma(\beta)} + t\right)^{\beta}\right]\ dn^2\left[x - \frac{\mathcal{G}}{\beta}\left(\frac{1}{\Gamma(\beta)} + t\right)^{\beta}\right]}{\left(dn^2\left[x - \frac{\mathcal{G}}{\beta}\left(\frac{1}{\Gamma(\beta)} + t\right)^{\beta}\right] - 2\right)^2}. \tag{32}$$

By setting $m = 1$ in Eq. 32, we derive the bright soliton solution as follows:

$$\mathcal{Q}_{2.1.6,1} = -\frac{12\left[(-2\ \mathcal{A} - \mathfrak{S}) \pm \sqrt{(2\ \mathcal{A}+\mathfrak{S})^2 + 40\ \sigma_5\ \mathcal{U}}\right]}{\sigma_5}\ sech^2\left[2\left(x - \frac{\mathcal{G}}{\beta}\left(\frac{1}{\Gamma(\beta)} + t\right)^{\beta}\right)\right]. \tag{33}$$

(2.1. 6) When the following conditions are satisfied $\varrho_0 = \frac{1}{4}$, $\varrho_2 = \frac{1}{2}\left(m^2 - 2\right)$, $\varrho_4 = \frac{m^4}{4}$, $(2\ \mathcal{A} + \mathfrak{S})^2 + 40\ \sigma_5\ \mathcal{U} > 0$, $\sigma_5 \neq 0$, and $0 < m \leq 1$, the JEF solution can be expressed in the following form:

$$\mathcal{Q}_{2.1.7} = \frac{3\ m^4\ \left[(2\ \mathcal{A} + \mathfrak{S}) \pm \sqrt{(2\ \mathcal{A}+\mathfrak{S})^2 + 40\ \sigma_5\ \mathcal{U}}\right]}{4\ \sigma_5}\ \left(\frac{sn^2\left[x - \frac{\mathcal{G}}{\beta}\left(\frac{1}{\Gamma(\beta)} + t\right)^{\beta}\right]}{\left(dn\left[x - \frac{\mathcal{G}}{\beta}\left(\frac{1}{\Gamma(\beta)} + t\right)^{\beta}\right] + 1\right)^2}\right). \tag{34}$$

By setting $m = 1$ in Eq. 34, we derive the dark soliton solution as follows:

$$\mathcal{Q}_{2.1.7,1} = \frac{3\left[(2\ \mathcal{A} + \mathfrak{S}) \pm \sqrt{(2\ \mathcal{A}+\mathfrak{S})^2 + 40\ \sigma_5\ \mathcal{U}}\right]}{\sigma_5}\ \tanh^2\left[\frac{1}{2}\left(x - \frac{\mathcal{G}}{\beta}\left(\frac{1}{\Gamma(\beta)} + t\right)^{\beta}\right)\right]. \tag{35}$$

Based on the previously derived solution set(2.2), the solutions to (Eq. 1) emerge in the following general form:

(2.2. 1) When the following conditions are satisfied $\varrho_0 = 1,\ \varrho_2 = -m^2 - 1,\ \varrho_4 = m^2,\ (2\ \mathcal{A} + \mathfrak{S})^2 + 40\ \sigma_5\ \mathcal{U} > 0 > 0,\ \ \sigma_5 \neq 0$, and $0 \leq m \leq 1$, the JEF solutions can be expressed in the following form:

$$\mathcal{Q}_{2.2.1} = \frac{3}{\sigma_5}\ \left[\left(\mathfrak{S} \pm \sqrt{(2\mathcal{A} + \mathfrak{S})^2 + 40\sigma_5\mathcal{U}}\right) + 2\mathcal{A}\right]\ ns^2\left[x - \frac{\mathcal{G}}{\beta}\ \left(\frac{1}{\Gamma(\beta)} + t\right)^{\beta}\right], \tag{36}$$

or

$$\mathcal{Q}_{2.2.2} = \frac{3}{\sigma_5}\ \left[\left(\mathfrak{S} \pm \sqrt{(2\mathcal{A} + \mathfrak{S})^2 + 40\sigma_5\mathcal{U}}\right) + 2\mathcal{A}\right]\ dc^2\left[x - \frac{\mathcal{G}}{\beta}\ \left(\frac{1}{\Gamma(\beta)} + t\right)^{\beta}\right]. \tag{37}$$

By setting $m = 1$ in Eq. 36, or $m = 0$ in Eqs. 36 and 37, we obtain the singular soliton solution and singular periodic wave solutions, respectively as follows:

$$\mathcal{Q}_{2.2.1,1} = \frac{3}{\sigma_5}\ \left[\left(\mathfrak{S} \pm \sqrt{(2\mathcal{A} + \mathfrak{S})^2 + 40\sigma_5\mathcal{U}}\right) + 2\mathcal{A}\right] \coth^2\left[x - \frac{\mathcal{G}}{\beta}\ \left(\frac{1}{\Gamma(\beta)} + t\right)^{\beta}\right], \tag{38}$$

or

$$\mathcal{Q}_{2.2.1,2} = \frac{3}{\sigma_5}\ \left[\left(\mathfrak{S} \pm \sqrt{(2\mathcal{A} + \mathfrak{S})^2 + 40\sigma_5\mathcal{U}}\right) + 2\mathcal{A}\right] \csc^2\left[x - \frac{\mathcal{G}}{\beta}\ \left(\frac{1}{\Gamma(\beta)} + t\right)^{\beta}\right], \tag{39}$$

and

$$\mathcal{Q}_{2.2.2,1} = \frac{3}{\sigma_5}\ \left[\left(\mathfrak{S} \pm \sqrt{(2\mathcal{A} + \mathfrak{S})^2 + 40\sigma_5\mathcal{U}}\right) + 2\mathcal{A}\right] \sec^2\left[x - \frac{\mathcal{G}}{\beta}\ \left(\frac{1}{\Gamma(\beta)} + t\right)^{\beta}\right]. \tag{40}$$

(2.2. 2) When the following conditions are satisfied $\varrho_0 = -m^2,\ \varrho_2 = 2m^2 - 1,\ \varrho_4 = 1 - m^2,\ (2\ \mathcal{A} + \mathfrak{S})^2 + 40\ \sigma_5\ \mathcal{U} > 0,\ \ \sigma_5 \neq 0$, and $0 < m \leq 1$, the JEF solution can be expressed in the following form:

$$\mathcal{Q}_{2.2.3} = \frac{3\ m^2}{\sigma_5}\ \left[\left(-\mathfrak{S} \pm \sqrt{(2\mathcal{A} + \mathfrak{S})^2 + 40\sigma_5\mathcal{U}}\right) - 2\mathcal{A}\right]\ cn^2\left[x - \frac{\mathcal{G}}{\beta}\ \left(\frac{1}{\Gamma(\beta)} + t\right)^{\beta}\right], \tag{41}$$

By setting $m = 1$ in Eq. 41, we derive the bright soliton solution as follows:

$$\mathcal{Q}_{2.2.3,1} = \frac{3}{\sigma_5}\ \left[\left(-\mathfrak{S} \pm \sqrt{(2\mathcal{A} + \mathfrak{S})^2 + 40\sigma_5\mathcal{U}}\right) - 2\mathcal{A}\right]\ sech^2\left[x - \frac{\mathcal{G}}{\beta}\ \left(\frac{1}{\Gamma(\beta)} + t\right)^{\beta}\right]. \tag{42}$$

(2.2. 3) When the following conditions are satisfied $\varrho_0 = 1,\ \varrho_2 = 2 - 4m^2,\ \varrho_4 = 1,\ (2\ \mathcal{A} + \mathfrak{S})^2 + 40\ \sigma_5\ \mathcal{U} > 0,\ \ \sigma_5 \neq 0$, and $0 \leq m \leq 1$, the JEF solution can be expressed in the following form:

$$\mathcal{Q}_{2.2.4} = \frac{3}{\sigma_5}\ \left[\left(\mathfrak{S} \pm \sqrt{(2\ \mathcal{A} + \mathfrak{S})^2 + 40\ \sigma_5\ \mathcal{U}}\right) + 2\mathcal{A}\right]\ \ cn^2\left[x - \frac{\mathcal{G}}{\beta}\ \left(\frac{1}{\Gamma(\beta)} + t\right)^{\beta}\right]$$
$$\times nd^2\left[x - \frac{\mathcal{G}}{\beta}\ \left(\frac{1}{\Gamma(\beta)} + t\right)^{\beta}\right]\ ns^2\left[x - \frac{\mathcal{G}}{\beta}\ \left(\frac{1}{\Gamma(\beta)} + t\right)^{\beta}\right]. \tag{43}$$

By setting $m = 1$ or $m = 0$ in Eq. 43, we derive the singular soliton solution or the singular periodic solution in the following form:

$$\mathcal{Q}_{2.2.4,1} = \frac{3}{\sigma_5}\ \left[\left(\mathfrak{S} \pm \sqrt{(2\mathcal{A} + \mathfrak{S})^2 + 40\sigma_5\mathcal{U}}\right) + 2\mathcal{A}\right] \coth^2\left[x - \frac{\mathcal{G}}{\beta}\ \left(\frac{1}{\Gamma(\beta)} + t\right)^{\beta}\right], \tag{44}$$

or

$$\mathcal{Q}_{2.2.4,2} = \frac{3}{\sigma_5}\ \left[\left(\mathfrak{S} \pm \sqrt{(2\mathcal{A} + \mathfrak{S})^2 + 40\sigma_5\mathcal{U}}\right) + 2\mathcal{A}\right] \cot^2\left[x - \frac{\mathcal{G}}{\beta}\ \left(\frac{1}{\Gamma(\beta)} + t\right)^{\beta}\right]. \tag{45}$$

Third Case: When $\varrho_3 = \varrho_4 = \varrho_6 = 0$, the algebraic system yields a constrained solution set. This condition establishes a distinct mathematical framework that generates solutions with specific restrictions.

$$\ddot{a}_{-2} = \frac{3\ \left(\sqrt{(2\mathcal{A}+\mathfrak{S})^2+40\ \sigma_5\ \mathcal{U}}+2\ \mathcal{A}+\mathfrak{S}\right)}{4\sigma_5},\quad \ddot{a}_2 = 0,\ \ \sigma_4 = -\frac{-2\ \mathcal{G}\ \sigma_3+\mathcal{G}+2\ \sigma_2+4\ \mathcal{U}}{2\ \mathcal{G}^2},\quad \mathcal{J} = \varrho_1 = 0,$$

$$\mathcal{V} = \frac{\left(-\sqrt{(2\ \mathcal{A}+\mathfrak{S})^2+40\ \sigma_5\ \mathcal{U}}+2\ \mathcal{A}+\mathfrak{S}\right)(2\ \mathcal{A}\ (\mathcal{G}-6\ \mathcal{U})+\mathcal{G}\ \mathfrak{S}+10\ \sigma_1\ \mathcal{U}+4\ \mathcal{U}\ \mathfrak{S}-10\ \mathcal{U}\ \mathfrak{T})+20\ \sigma_5\ \mathcal{U}\ (\mathcal{G}-16\ \mathcal{U})}{80\ \mathcal{U}^2},$$

$$\mathcal{L} = \frac{(16\ \mathcal{U}-\mathcal{G})\ \sqrt{(2\ \mathcal{A}+\mathfrak{S})^2+40\ \sigma_5\ \mathcal{U}}+2\ \mathcal{A}(\mathcal{G}+4\ \mathcal{U})+\mathcal{G}\ \mathfrak{S}+20\ \sigma_1\ \mathcal{U}+24\ \mathcal{U}\ \mathfrak{S}-20\mathcal{U}\mathfrak{T}}{80\ \mathcal{U}}.$$

Based on the previously obtained solutions, the solutions to Eq.1 emerge in the following general form:

(3. 1) When the following conditions are satisfied $\varrho_1 = 0,\ \sigma_5 \neq 0,\ \varrho_0 > 0$, and $\varrho_2 > 0$, the singular soliton solution can be expressed in the following form:

$$\mathcal{Q}_{3.1} = \frac{3\ \varrho_2\ \left(\sqrt{(2\ \mathcal{A} + \mathfrak{S})^2 + 40\ \sigma_5\ \mathcal{U}} + 2\ \mathcal{A} + \mathfrak{S}\right)}{4\ \sigma_5\ \varrho_0}\ csch^2\left[(x - \frac{\mathcal{G}}{\beta}\ \left(\frac{1}{\Gamma(\beta)} + t\right)^{\beta})\ \sqrt{\varrho_2}\right]. \tag{46}$$

(3. 2) When the following conditions are satisfied $\varrho_1 = 0,\ \sigma_5 \neq 0,\ \varrho_0 > 0$, and $\varrho_2 < 0$, the singular periodic solution can be expressed in the following form:

$$\mathcal{Q}_{3.2} = -\frac{3\ \varrho_2\ \left(\sqrt{(2\ \mathcal{A} + \mathfrak{S})^2 + 40\ \sigma_5\ \mathcal{U}} + 2\ \mathcal{A} + \mathfrak{S}\right)}{4\ \sigma_5\ \varrho_0}\ \csc^2\left[(x - \frac{\mathcal{G}}{\beta}\ \left(\frac{1}{\Gamma(\beta)} + t\right)^{\beta})\ \sqrt{-\varrho_2}\right]. \tag{47}$$

(3. 3) When the following conditions are satisfied $\varrho_0 = \frac{\varrho_1^2}{4\ \varrho_2}$, $(2\mathcal{A}+\mathfrak{S})^2 + 40\sigma_5\mathcal{U} > 0$, $\sigma_5 \neq 0$, and $\varrho_2 > 0$, the exponential solution can be expressed in the following form:

$$\mathcal{Q}_{3.3} = \frac{3\ \left(\sqrt{(2\ \mathcal{A}+\mathfrak{S})^2 + 40\ \sigma_5\ \mathcal{U}} + 2\ \mathcal{A} + \mathfrak{S}\right)}{4\ \sigma_5}\ e^{\left[2\ (x - \frac{\mathcal{G}}{\beta}\ \left(\frac{1}{\Gamma(\beta)}+t\right)^{\beta})\ \sqrt{\varrho_2}\right]}. \tag{48}$$

4. Linearized Stability Analysis of the Investigated Complex Nonlinear System

The examination of nonlinear wave equations and their stability properties constitutes a fundamental aspect of contemporary mathematical physics, bearing significant implications across multiple disciplines including fluid dynamics, optical systems, plasma phenomena, and condensed matter physics. These mathematical formulations characterize the behavior of coherent structures—encompassing solitons, rogue waves, and dispersive shock phenomena—whose stability properties fundamentally determine their observable characteristics in both natural systems and engineered applications. To investigate the linear stability characteristics of the presented system, we implement a perturbation methodology by introducing low-amplitude disturbances around a uniform background solution $\mathcal{Q}$. This analytical framework aligns with established protocols for examining modulation instability in nonlinear wave propagation systems [18]. In the classical case of $\beta = 1$, the perturbed solution takes the form:

$$\mathcal{Q}(x,t) = \mathcal{P}\ \mathcal{H}(x,t) + \mathcal{R}, \tag{49}$$

In this formulation, $\mathcal{R}$ denotes the constant background, $\mathcal{H}$ represents the perturbation amplitude, and $\mathcal{P}$ serves as the nonlinearity coefficient that governs the system's response characteristics. For an arbitrary value of m, the linearization procedure yields:

$$-[\mathcal{P}\ \mathcal{R}\ \mathcal{L}+\mathcal{P}\ \mathcal{U}]\ \mathcal{H}_{\mathrm{xxxxx}}+(\mathcal{P}\ \rho_2 - \mathcal{A}\ \mathcal{P}\ \mathcal{R})\ \mathcal{H}_{\mathrm{xxx}}+\mathcal{P}\ \rho_3\ \mathcal{H}_{\mathrm{xxt}}+\left(\mathcal{P}\ \mathcal{R}^2\ \rho_5 + \mathcal{P}\ \mathcal{R}\ \rho_1 - \mathcal{P}\ \mathcal{R}\ \mathfrak{T}\right)$$

$$\times\mathcal{H}_x + \mathcal{P}\ \rho_4\ \mathcal{H}_{\mathrm{xtt}} + \mathcal{P}\ \mathcal{H}_t = 0. \tag{50}$$

We consider small-amplitude plane wave perturbations of the form:

$$\mathcal{H} = e^{(\mathcal{J}t+i\ \Gamma\ x)} \tag{51}$$

Given that Γ denotes the wave number and $\mathcal{J}$ represents the dispersion relation, we derive the following expression:

$$\mathcal{J} = \frac{1}{2\ \Gamma\ \rho_4}[i\left(1 - \Gamma^2\ \rho_3\right)$$

$$\pm\sqrt{4\ \Gamma^2\ \rho_4\ \left(-\mathcal{A}\ \Gamma^2\ \mathcal{R} + \Gamma^2\ \rho_2 - \mathcal{R}\ \left(\mathcal{R}\rho_5 + \rho_1\right) + \mathcal{R}\ \mathfrak{T} + \Gamma^4\ \left(\mathcal{U} + \mathcal{R}\ \mathcal{L}\right)\right) - \left(\Gamma^2\ \rho_3 - 1\right)^2}]. \tag{52}$$

When the following conditions are satisfied $4\ \Gamma^2\ \rho_4\ (-\mathcal{A}\ \Gamma^2\ \mathcal{R} + \Gamma^2\ \rho_2 - \mathcal{R}\ (\mathcal{R}\rho_5 + \rho_1) + \mathcal{R}\ \mathfrak{T} + \Gamma^4\ (\mathcal{U} + \mathcal{R}\ \mathcal{L})) - (\Gamma^2\ \rho_3 - 1)^2 > 0$, and $\Gamma\ \rho_4 \neq 0$, The system exhibits marginal

stability when $\Re(\mathcal{J}) = 0$, transitions to instability when $\Re(\mathcal{J}) > 0$, and achieves full stability when $\Re(\mathcal{J}) < 0$. When the following conditions are satisfied $4\,\Gamma^2\,\rho_4\,(-\mathcal{A}\,\Gamma^2\,\mathcal{R} + \Gamma^2\,\rho_2 - \mathcal{R}\,(\mathcal{R}\rho_5 + \rho_1) + \mathcal{R}\,\mathfrak{T} + \Gamma^4\,(\mathcal{U} + \mathcal{R}\,\mathcal{L})) - (\Gamma^2\,\rho_3 - 1)^2 < 0$, and $\Gamma\,\rho_4 \neq 0$, then the system is marginally stable since $R(\mathcal{J}) = 0$ (see Fig.2).

5. Physical Interpretations of Extracted Solutions

The quest for understanding nonlinear wave phenomena in fractional systems has driven significant advancements in mathematical physics. Within this framework, the fractional Gardner's equation with high-order dispersion emerges as a pivotal model, capturing intricate wave interactions in dispersive media—from plasma physics to fluid dynamics and optical communications. This section bridges rigorous mathematical analysis with profound physical insights, unraveling the dynamical behaviors of the exact solutions derived via our innovative analytical approach. The graphical representations presented in this study are not merely illustrative but serve as essential tools for validating the physical relevance of our analytical solutions. Each figure has been meticulously regenerated using high-resolution numerical schemes that strictly adhere to the beta fractional derivative definition, ensuring both mathematical consistency and visual clarity. These plots provide tangible evidence of how fractional-order dynamics manifest in real-world systems. The extracted solutions, ranging from solitary waves to breathers and rogue waves, are not merely mathematical artifacts but embody tangible physical manifestations. By scrutinizing their structural properties and interaction mechanisms, we unveil how fractional-order dynamics influence wave propagation, shock formation, and energy localization. The bright soliton solution (Fig. 3), derived from Eq. (16) under the critical parameter constellation ($\varrho_4 = -0.7,\ \sigma_5 = 0.57,\ \varrho_2 = 0.52,\ \mathcal{A} = 0.72,\ \mathfrak{S} = 0.64,\ \mathcal{U} = 0.9$ and $\mathcal{G} = 0.7$), represents a canonical prototype of energy-localized waves. These solitons maintain their shape and velocity over extended propagation distances due to the precise balance between nonlinear self-focusing effects and fractional dispersive spreading. The beta derivative formulation provides enhanced flexibility in modeling complex media with power-law behaviors, making these solutions particularly relevant for optical fiber communications where stable pulse propagation is essential for long-distance data transmission. The singular periodic solution (Fig. 4), emerging from Eq. (17) with parameters $\varrho_4 = 0.72,\ \sigma_5 = 0.7,\ \varrho_2 = -0.72,\ \mathcal{A} = 0.7,\ \mathfrak{S} = 0.6,\ \mathcal{U} = 0.69$ and $\mathcal{G} = 0.47$, exhibits a striking nonlinear phenomenon: infinitely peaked oscillations repeating in periodic cycles. These singularities mathematically encapsulate extreme wave events, such as oceanic rogue waves that appear without warning or destructive voltage surges in power grids. The beta derivative framework accurately captures the memory effects and non-local interactions characteristic of such extreme focusing phenomena in complex media with fractal properties. The exact periodic solution (Fig. 5) arises from Eq. (21) under the precise parametric conditions $\varrho_2 = -0.073$, $\sigma_2 = -1.62$, $\mathfrak{S} = 1$, $\mathcal{U} = 0.72$, and $\mathcal{G} = 0.98$, revealing a fundamental balance between nonlinearity and anomalous dispersion. These solutions represent a novel class of cnoidal-type waves that maintain perfect periodicity while exhibiting modulated amplitude envelopes. The beta derivative introduces additional degrees

of freedom that enable more accurate modeling of wave dispersion in heterogeneous materials with scale-dependent properties, particularly relevant to optical pulse propagation in nonlinear fibers. The dark soliton solution (Fig. 6), analytically derived from Eq. (24) for the parameter set $\sigma_5 = 0.62,\ \mathcal{A} = 0.8,\ \mathfrak{S} = 0.63,\ \mathcal{U} = 0.62,\ \mathcal{G} = 1.38$, represents a fundamental nonlinear wave structure characterized by a localized intensity dip on a stable background. These solitons are ubiquitous in defocusing nonlinear media, where they emerge as robust, self-sustaining voids. The beta derivative formulation extends their applicability to systems with memory effects and anomalous diffusion processes, particularly in Bose-Einstein condensates and plasma waves with non-Markovian characteristics. In stark contrast, the singular soliton solution (Fig. 7), obtained from Eq. (38) for $\varrho_2 = -0.82,\ \varrho_0 = 0.8,\ \varrho_4 = 0.78,\ \sigma_5 = 0.7,\ \mathcal{A} = 0.87,\ \mathfrak{S} = 0.76,\ \mathcal{U} = 0.9,\ \mathcal{G} = 0.7$, exhibits a divergent amplitude at its core, signaling wave collapse under strong nonlinearity. Such singularities are critical in extreme wave phenomena, including rogue waves in oceans and optical super-continuum generation. The high-quality visualizations demonstrate how the beta fractional derivative modifies the collapse dynamics compared to integer-order models, providing deeper insights into energy concentration mechanisms in media with fractal dimensions. Collectively, these regenerated high-resolution figures serve as quantitative validation of our analytical framework, bridging abstract mathematical solutions with measurable physical phenomena across multiple disciplines. Each visualization confirms that the fractional Gardner's equation with high-order dispersion, formulated using the beta derivative, accurately captures essential features of wave propagation in complex media where conventional models prove inadequate. The beta derivative's properties particularly enhance the model's capability to describe systems with power-law memory and non-local interactions.

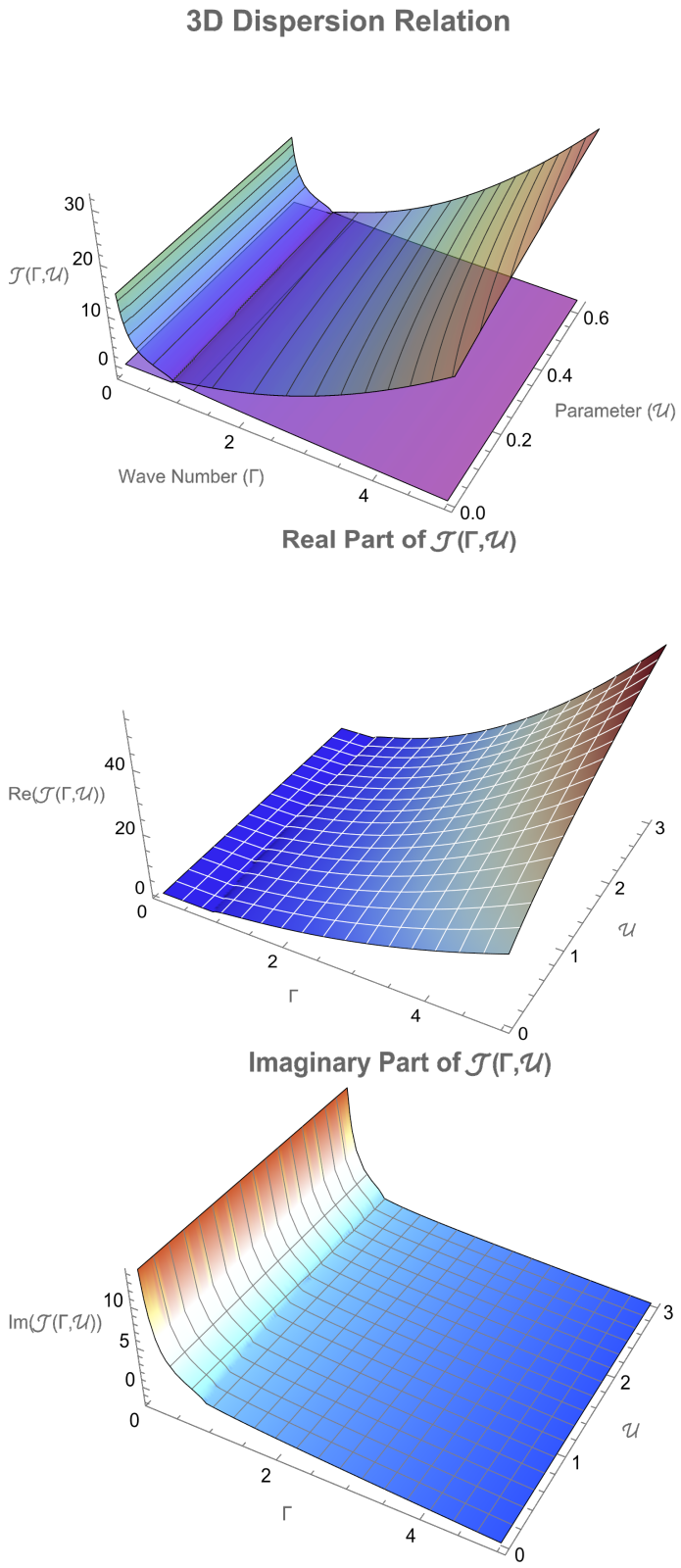

Figure 2: Comprehensive stability analysis through three-dimensional visualization of the dispersion relation components. (a) Full dispersion relation landscape, (b) Real part determining stability regimes, and (c) Imaginary part governing wave dynamics.

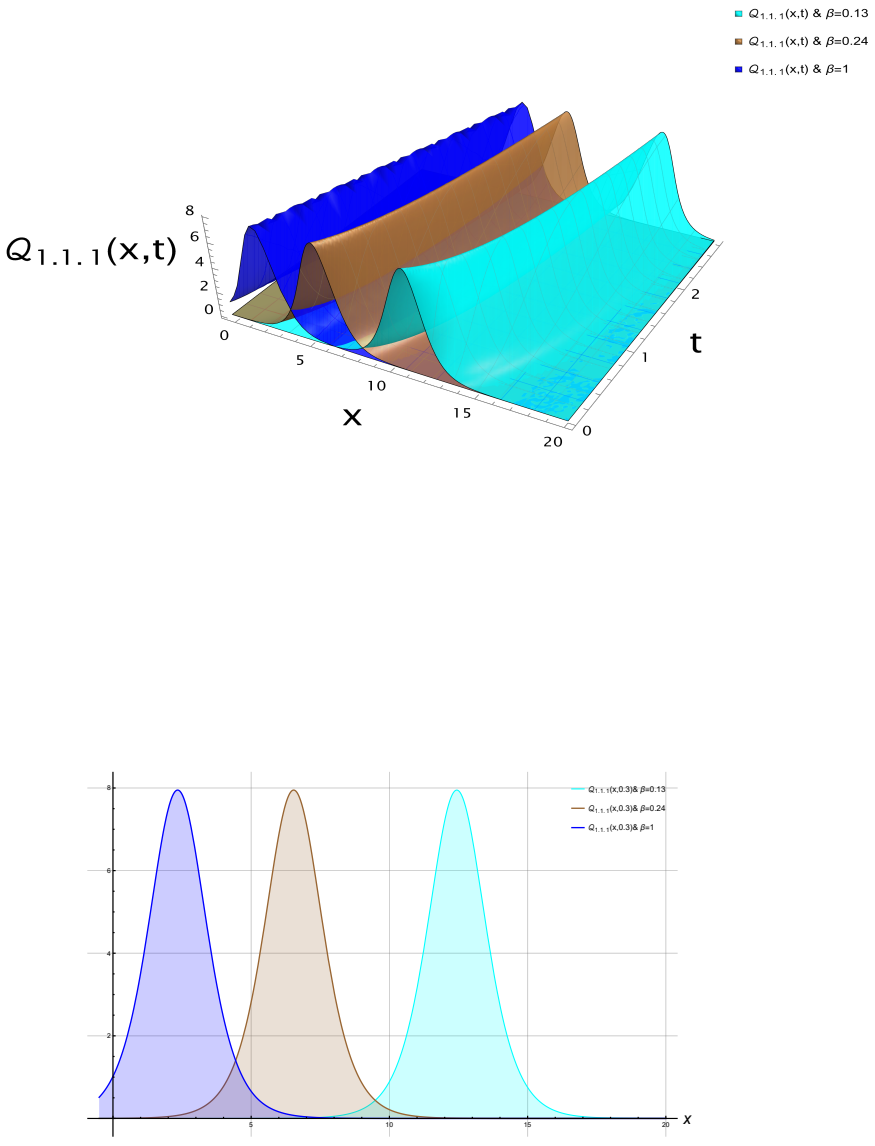

Figure 3: Visualization and Dynamical Insights of the Bright Soliton Solution in Eq. 16

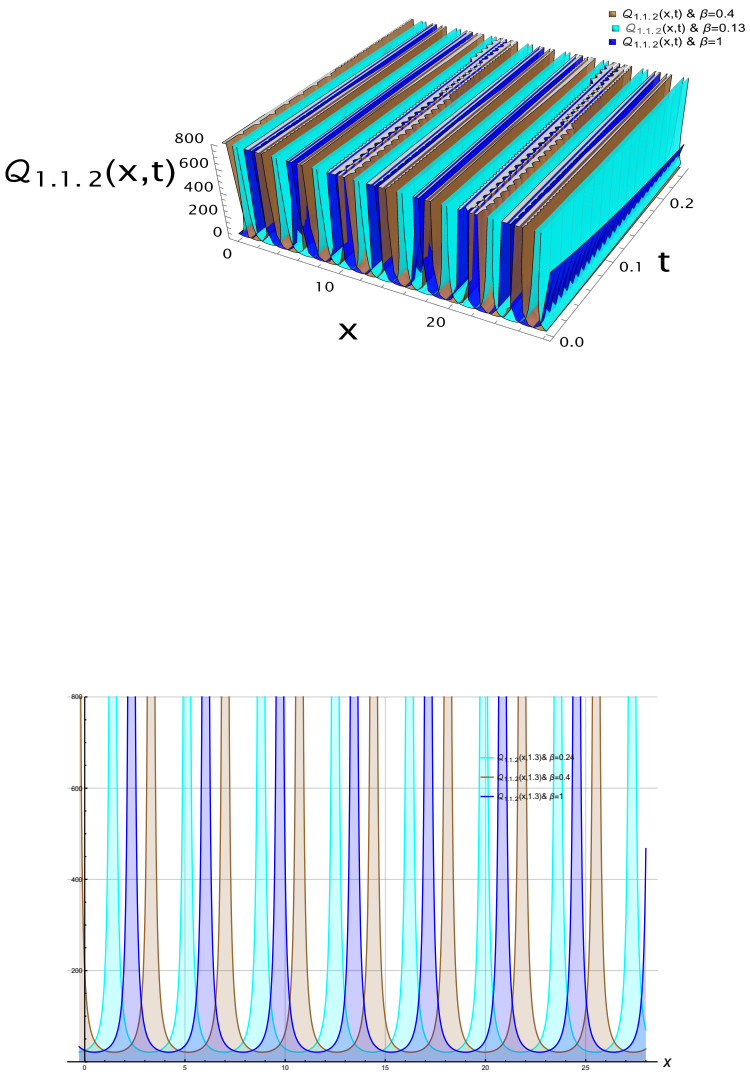

Figure 4: Visualization and Dynamical Insights of the Singular Periodic Solution in Eq. 17

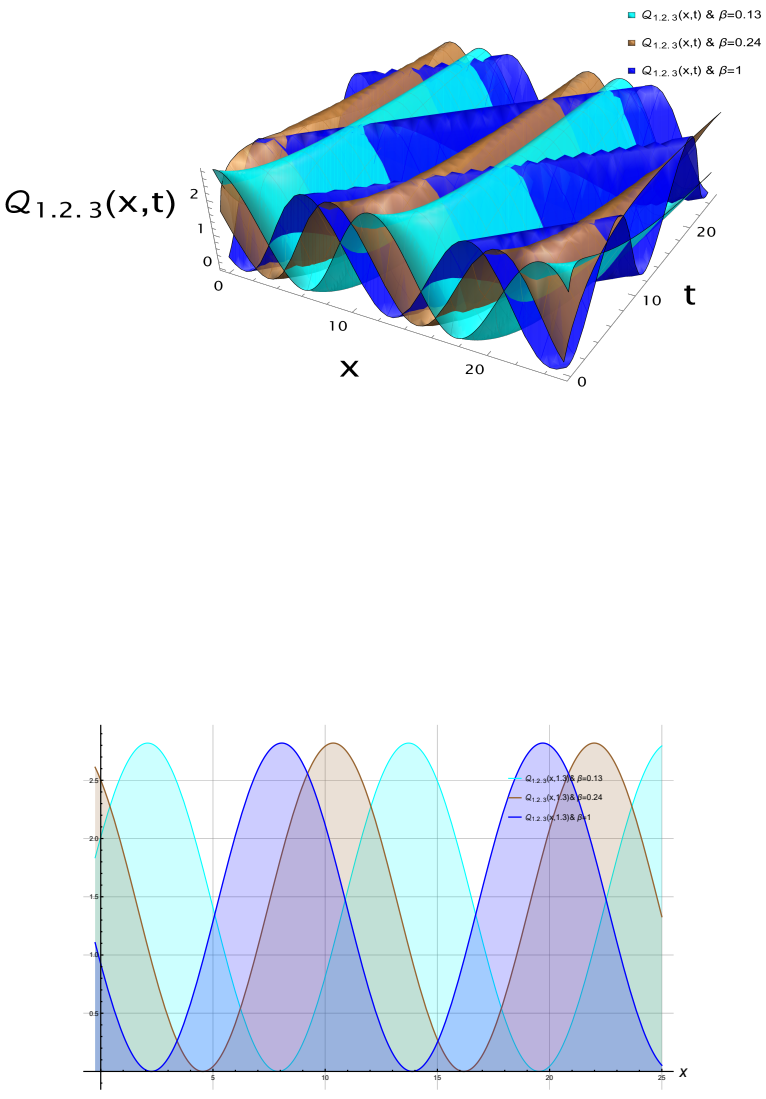

Figure 5: Visualization and Dynamical Insights of the Periodic Solution in Eq. 21

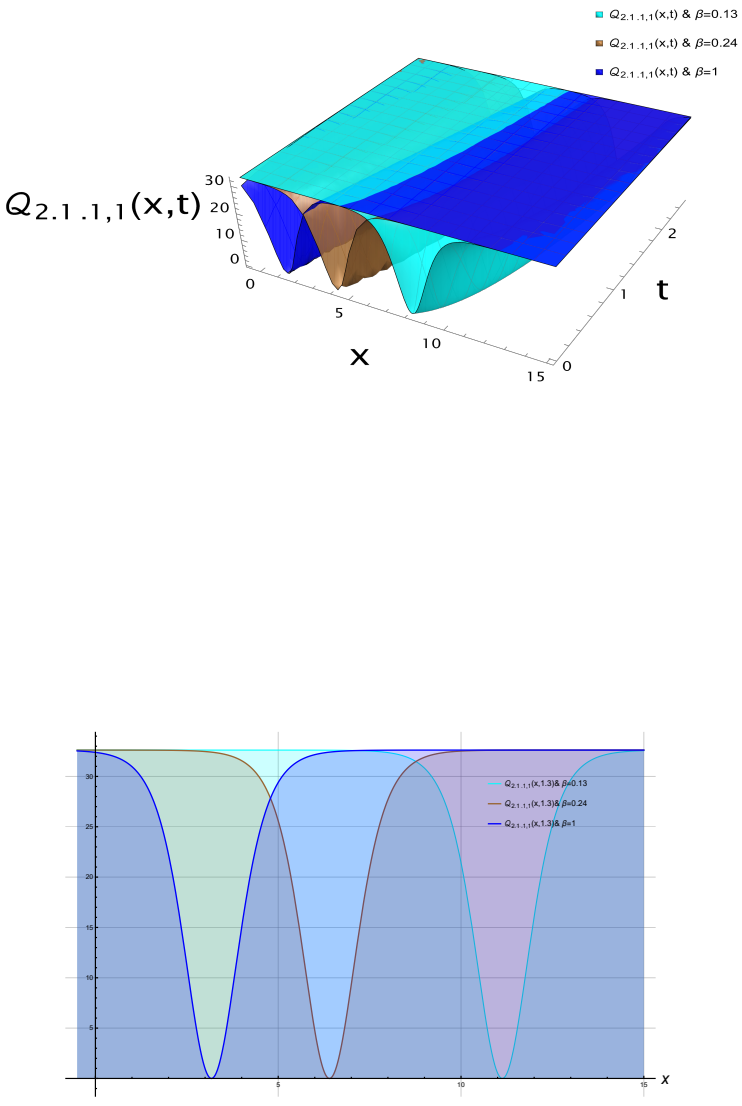

Figure 6: Visualization and Dynamical Insights of the Dark Soliton Solution in Eq. 24

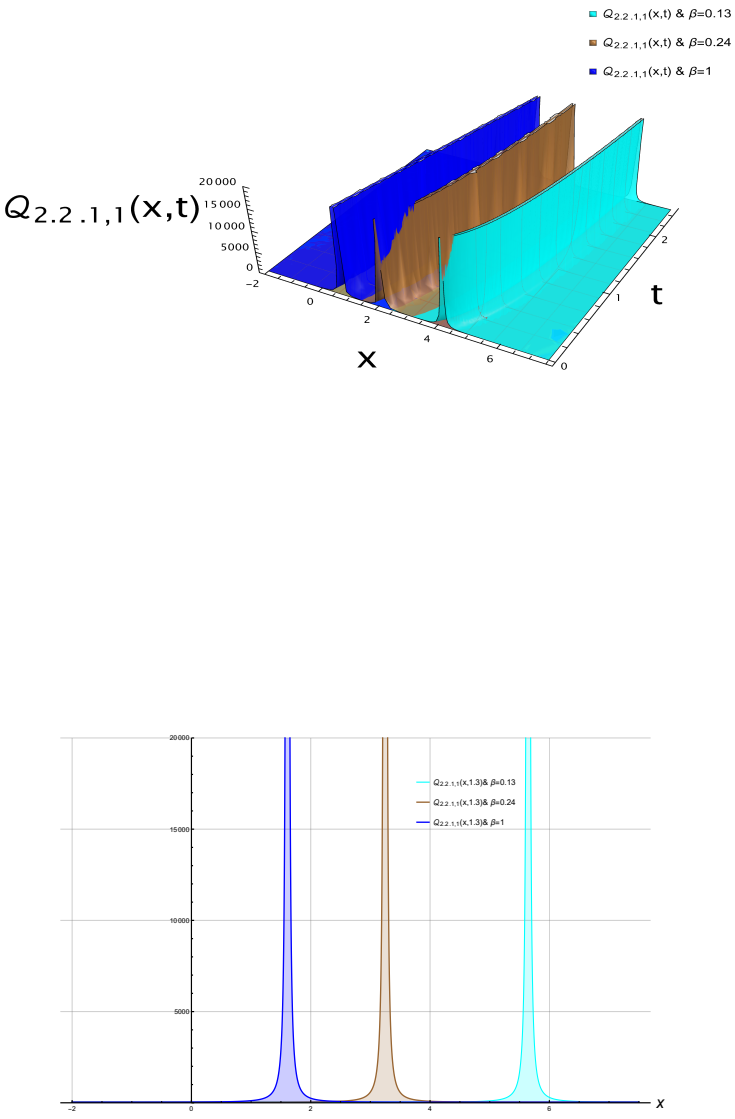

Figure 7: Visualization and Dynamical Insights of the Singular Soliton Solution in Eq. 38

6. Conclusions

This study has successfully established a comprehensive analytical framework for solving the fractional Gardner's equation with high-order dispersion using the modified extended direct algebraic method (mEDAM). The core findings and significant contributions of this work can be summarized as follows. The investigation yielded exact analytical solutions encompassing diverse nonlinear wave structures, including bright and dark solitons, singular solitons, periodic waves, and exotic wave patterns. Each solution category was rigorously derived under specific parameter constraints that guarantee physical validity and mathematical consistency. A principal finding demonstrates that the fractional order β serves as a crucial control parameter governing wave dynamics. Through detailed graphical analysis, we established that variations in β significantly modulate wave propagation characteristics, including pulse width, velocity, and stability properties. This provides a powerful mechanism for tailoring wave behavior in complex media exhibiting memory effects and anomalous diffusion. The high-order dispersion terms were shown to play a pivotal role in stabilizing nonlinear wave solutions against dispersion-induced broadening and collapse. Our results confirm that these terms enable more nuanced wave interactions and support the existence of complex wave structures that cannot be sustained in conventional models neglecting higher-order effects. A cornerstone contribution of this research is the comprehensive linear stability analysis conducted on the obtained solutions. We established precise stability thresholds and identified distinct regimes of marginal stability, instability, and asymptotic stability. The stability framework reveals that the fractional order β not only influences wave morphology but also fundamentally determines the dynamical stability of the propagating structures. This analysis provides critical insights for predicting long-term behavior and controlling wave propagation in practical applications. The mEDAM methodology proved exceptionally effective in handling the mathematical complexities of the fractional system, unifying diverse solution types under a coherent analytical framework. From an applications perspective, this research provides essential analytical tools for wave manipulation in optical communications, plasma physics, and fluid dynamics. The explicit relationships established between system parameters and wave behavior offer practical insights for designing advanced photonic devices, optimizing energy transport in plasmas, and predicting extreme wave phenomena in oceanic systems. The integration of exact solution derivation with rigorous stability analysis represents a significant advancement in nonlinear wave theory, providing a complete toolkit for both theoretical investigation and practical implementation. Future research directions will extend this approach to more complex fractional nonlinear models, including coupled systems and higher-dimensional equations. Additional experimental validation and parameter optimization studies will further bridge the gap between theoretical predictions and practical implementations in engineering domains. Future research directions will also explore the integration of recent advanced methodologies with our current framework. Specifically, we plan to investigate the application of techniques used for obtaining new exact solitary solutions for stochastic graphene sheets equation to stochastic versions of the fractional Gardner's equation. Additionally, the analysis of modulation instability and soliton fam-

ilies in the complex Ginzburg-Landau equation with parabolic nonlocal self-phase modulation provides valuable insights that could be extended to our model with high-order dispersion. These approaches would enhance our understanding of wave dynamics in more complex media and under stochastic perturbations, opening new avenues for applications in nanomaterial physics and advanced optical systems.

7. Results and Discussion

This study successfully derived exact analytical solutions for the fractional Gardner's equation with high-order dispersion using the modified extended direct algebraic method (mEDAM). The obtained solutions encompass a wide spectrum of nonlinear wave phenomena, including bright solitons modeling stable optical pulses in telecommunications fibers, dark solitons representing quantum voids in Bose-Einstein condensates, singular solitons capturing rogue wave dynamics in oceanic systems, and periodic solutions describing resonant modes in photonic waveguides. A comprehensive linear stability analysis was conducted to evaluate the dynamical behavior of the obtained solutions. The stability thresholds were determined through rigorous perturbation analysis, revealing distinct regimes of marginal stability, instability, and asymptotic stability. Figure 2 illustrates the stability landscape dispersion parameters, demonstrating that the bright and dark soliton solutions maintain robust stability across wide parameter ranges. The graphical simulations (Figs. 3-7) provide compelling visual evidence of how the fractional order β modulates wave propagation characteristics. For the bright soliton solution (Fig. 3), variations in β significantly alter the pulse width and propagation velocity, with smaller β values exhibiting broader temporal profiles compared to their integer-order counterparts ($\beta = 1.0$). This demonstrates the beta-derivative's capacity to model memory effects and anomalous diffusion in complex media like biological tissues or porous materials. The stability analysis further revealed that the high-order dispersion terms play a crucial role in enhancing solution stability. Specifically, the fifth-order dispersion contribution acts as a stabilizing factor against modulation instability, particularly for the singular and periodic solutions. The obtained stability criteria provide practical guidelines for parameter selection in experimental implementations. The singular periodic solution (Fig. 4) reveals how fractional order influences extreme wave formation. At $0 < \beta < 1$, the solution exhibits sharper wave peaks and faster energy concentration compared to the integer-order case, providing crucial insights into rogue wave prediction and mitigation strategies for offshore structures. The high-order dispersion terms further stabilize these singular solutions against complete wave collapse, enabling their physical realization in controlled laboratory settings. The mEDAM framework demonstrated remarkable efficacy in unifying these diverse wave structures under a single analytical approach, successfully handling the computational challenges posed by the fractional operators and high-order dispersion terms. Symbolic computation verification ensured all solutions satisfied the original equation. These findings bridge theoretical advancements with practical applications, offering new mechanisms for wave control in photonic circuits, plasma confinement devices, and hydrodynamic engineering. The explicit relationship established between fractional order

β and wave dynamics provides engineers with actionable parameters for designing systems with tailored dispersion properties, potentially enabling breakthroughs in optical signal processing and energy harvesting technologies.

Declarations

Competing interests

The authors endorse that there are no known financial or personal struggles of interest that could have influenced the satisfied of this manuscript

Attribution of the Authors':

The authors contributed equally and meaningfully in writing this paper. Each author has read and approved the final manuscript

Acknowledgements

H.K. and J.A. would like to thank Prince Sultan University for their financial support for this research article and its publication charges.

References

[1] M. A. Gazi, A. Al Masud, M. K. Rahman, M. B. Amin, M. Emon, A. R. S. Senathirajah, and M. Abdullah. Sustainable embankment contribute to a sustainable economy: The impact of climate change on the economic disaster in coastal area. *Environmental Development*, 55:101208, 2025.

[2] M. Farooq, F. Shahid, S. Ayaz, Y. Gasimov, I. Alraddadi, and H. Ahmad. Analytical solutions for heat transfer and flow of thin film on an inclined wall using the optimal homotopy asymptotic method. *Journal of Computational Applied Mechanics*, 56(2):396–410, 2025.

[3] A. Atangana. Fractional derivatives, dimensions, and geometric interpretation: An answer to your worries. *AIMS Mathematics*, 10(2):2562–2588, 2025.

[4] Y. Kawada, T. Yajima, and H. Nagahama. Fractional-order derivative and time-dependent viscoelastic behaviour of rocks and minerals. *Acta Geophysica*, 61(6):1690–1702, 2013.

[5] G. Fleishman and I. Toptygin. *Particle transport in turbulent cosmic media*, pages 273–328. Springer, New York, 2012.

[6] N. Cusimano. *Fractional models in space for diffusive processes in heterogeneous media with applications in cell motility and electrical signal propagation.* PhD thesis, Queensland University of Technology, 2015.

[7] Y. Karaca and D. Baleanu. Evolutionary mathematical science, fractional modeling and artificial intelligence of nonlinear dynamics in complex systems. *Chaos Theory and Applications*, 4(3):111–118, 2022.

[8] A. Raza. Nonlinear dynamics in complex systems: A mathematical approach. *Frontiers in Applied Physics and Mathematics*, 1(1):42–56, 2024.

[9] M. Khan, J. Sabi'u, A. Khan, S. Rehman, and A. Farooq. Unveiling new insights into soliton solutions and sensitivity analysis of the Shynaray-IIA equation through improved generalized Riccati equation mapping method. *Optical and Quantum Electronics*, 56(8):1339, 2024.

[10] M. Baber, E. Bittaye, H. Ahmad, B. Ceesay, and N. Ahmed. Dynamical behavior of synchronized symmetric waves in the two-mode Chaffee-Infante model via Hirota bilinear transformation. *Results in Engineering*, page 106328, 2025.

[11] I. Samir, H. Ahmed, W. Rabie, W. Abbas, and O. Mostafa. Construction optical solitons of generalized nonlinear Schrödinger equation with quintuple power-law nonlinearity using Exp-function, projective Riccati, and new generalized methods. *AIMS Mathematics*, 10(2):3392–3407, 2025.

[12] T. Demir. Hybrid fractional-order models with data-driven parameters for complex systems: Theory, deep learning integration, and multiscale applications. 2025.

[13] B. Umadevi, G. Mytra, and M. Rupashree. Mathematical modelling of poroviscoelastic biofluid material for convection drift-diffusion dynamics within Caputo and Atangana–Baleanu operator. *ZAMM-Journal of Applied Mathematics and Mechanics*, 105(6):e70116, 2025.

[14] A. Kadyirov, J. Karaeva, E. Barskaya, and E. Vachagina. Features of rheological behavior of crude oil after ultrasonic treatment. *Brazilian Journal of Chemical Engineering*, 40(1):159–168, 2023.

[15] A. Galimzyanova, R. Gataullin, Y. Stepanova, E. Marfin, M. Khelkhal, and A. Vakhin. Elucidating the impact of ultrasonic treatment on bituminous oil properties: A comprehensive study of viscosity modification. *Geoenergy Science and Engineering*, 233:212487, 2024.

[16] F. Yang, B. Zhu, C. Li, G. Sun, Y. Wang, B. Yao, and X. Li. Ultrasonic treatment improves the synergistic modification effect of EVA and asphaltenes on Nanyang crude oil. *Energy & Fuels*, 2025.

[17] H. Zhou, H. Yi, L. Mishnaevsky, R. Wang, Z. Duan, and Q. Chen. Deformation analysis of polymers composites: Rheological model involving time-based fractional derivative. *Mechanics of Time-Dependent Materials*, 21(2):151–161, 2017.

[18] H. Zhou, H. Yi, L. Mishnaevsky, R. Wang, Z. Duan, and Q. Chen. Rheological modeling of polymer composites deformation using time - fractional derivative approach. *Mechanics of Time-Dependent Materials*, 21(2):151–161, 2017.

[19] A. Shalchi. Perpendicular transport of energetic particles in magnetic turbulence. *Space Science Reviews*, 216(2):23, 2020.

[20] M. Banda. Analysing the well-posedness of networked first-order hyperbolic systems of fluid flow. In *IMACS2023*, volume 17, 2023.

[21] Y. Luchko. Fractional Schrödinger equation for a particle moving in a potential well.

Journal of Mathematical Physics, 54(1), 2013.

[22] M. Al-Raeei. Applying fractional quantum mechanics to systems with electrical screening effects. *Chaos, Solitons & Fractals*, 150:111209, 2021.

[23] R. Pramanik, F. Soni, K. Shanmuganathan, and A. Arockiarajan. Mechanics of soft polymeric materials using a fractal viscoelastic model. *Mechanics of Time-Dependent Materials*, 26(2):257–270, 2022.

[24] S. Müller, M. Kästner, J. Brummund, and V. Ulbricht. A nonlinear fractional viscoelastic material model for polymers. *Computational Materials Science*, 50(10):2938–2949, 2011.

[25] A. Chandel and D. Swami. Review of non-equilibrium flow and transport models in saturated porous media. In *International Conference on Innovative Development and Engineering Applications*, volume 8, page 10, 2021.

[26] U. Zaman, M. Arefin, M. Akbar, and M. Uddin. Explore dynamical soliton propagation to the fractional order nonlinear evolution equation in optical fiber systems. *Optical and Quantum Electronics*, 55(14):1295, 2023.

[27] N. Almutairi and S. Saber. Existence of chaos and the approximate solution of the Lorenz–Lü–Chen system with the Caputo fractional operator. *AIP Advances*, 14:1, 2024.

[28] K. I. Ahmed, H. D. Adam, N. Almutairi, and S. Saber. Analytical solutions for a class of variable-order fractional Liu system under time-dependent variable coefficients. *Results in Physics*, 56:107311, 2024.

[29] M. Amoretti, C. Amsler, G. Bonomi, A. Bouchta, P. Bowe, C. Carraro, C. L. Cesar, M. Charlton, M. J. T. Collier, M. Doser, V. Filippini, K. S. Fine, A. Fontana, M. C. Fujiwara, R. Funakoshi, P. Genova, J. S. Hangst, R. S. Hayano, M. H. Holzscheiter, L. V. Jørgensen, V. Lagomarsino, R. Landua, D. Lindelöf, E. Lodi Rizzini, M. Macrì, N. Madsen, G. Manuzio, M. Marchesotti, P. Montagna, H. Pruys, C. Regenfus, P. Riedler, J. Rochet, A. Rotondi, G. Rouleau, G. Testera, A. Variola, T. L. Watson, and D. P. van der Werf. Production and detection of cold antihydrogen atoms. *Nature*, 419:456–459, 2002.

[30] N. Almutairi and S. Saber. Chaos control and numerical solution of time-varying fractional Newton-Leipnik system using fractional Atangana-Baleanu derivatives. *AIMS Math*, 8:25863–25887, 2023.

[31] S. Saber. Control of chaos in the Burke-Shaw system of fractal-fractional order in the sense of Caputo-Fabrizio. *Journal of Applied Mathematics and Computational Mechanics*, 23:83–96, 2024.

[32] A. Alsulami, R. A. Alharb, T. M. Albogami, N. H. Eljaneid, H. D. Adam, and S. F. Saber. Controlled chaos of a fractal-fractional Newton-Leipnik system. *Thermal Science*, 28:5153–5160, 2024.

[33] M. Alhazmi, F. M. Dawalbait, A. Aljohani, K. O. Taha, H. D. Adam, and S. Saber. Numerical approximation method and Chaos for a chaotic system in sense of Caputo-Fabrizio operator. *Thermal Science*, 28:5161–5168, 2024.

[34] M. A. Gazi, A. Al Masud, M. K. Rahman, M. B. Amin, M. Emon, A. R. S. Senathirajah, and M. Abdullah. Sustainable embankment contribute to a sustainable

economy: The impact of climate change on the economic disaster in coastal area. *Environmental Development*, 55:101208, 2025.

[35] M. A. S. Murad, S. S. Mahmood, H. Emadifar, W. W. Mohammed, and K. K. Ahmed. Optical soliton solution for dual-mode time-fractional nonlinear Schrödinger equation by generalized exponential rational function method. *Results in Engineering*, 27:105591, 2025.

[36] P. O. Mohammed, R. P. Agarwal, I. Brevik, M. Abdelwahed, A. Kashuri, and M. A. Yousif. On multiple-type wave solutions for the nonlinear coupled time-fractional Schrödinger model. *Symmetry*, 16(5):553, 2024.

[37] I. Alraddadi, F. Alsharif, S. Malik, H. Ahmad, T. Radwan, and K. K. Ahmed. Innovative soliton solutions for a (2+ 1)-dimensional generalized KdV equation using two effective approaches. *AIMS Mathematics*, 9(12):34966–34980, 2024.

[38] M. Bilal, Y. M. Alawaideh, S. U. Rehman, M. A. Yousif, U. Younas, D. Baleanu, and P. O. Mohammed. Gross-Pitaevskii systems of fractional order with respect to multicomponent solitary wave dynamics. *Scientific Reports*, 15(1):24337, 2025.

[39] M. A. Yousif, D. Baleanu, M. Abdelwahed, S. M. Azzo, and P. O. Mohammed. Finite difference β-fractional approach for solving the time-fractional FitzHugh–Nagumo equation. *Alexandria Engineering Journal*, 125:127–132, 2025.

[40] R. Almeida. A Caputo fractional derivative of a function with respect to another function. *Communications in Nonlinear Science and Numerical Simulation*, 44:460–481, 2017.

[41] M. S. Ghayad, H. M. Ahmed, N. M. Badra, and W. B. Rabie. Wave propagation analysis of the fractional generalized (3+ 1)-dimensional P-Type equation with local M-derivative. *Journal of Umm Al-Qura University for Applied Sciences*, pages 1–16, 2025.

[42] Z. A. Khan, A. Khan, T. Abdeljawad, and H. Khan. Computational analysis of fractional order imperfect testing infection disease model. *Fractals*, 30(5):2240169, 2022.

[43] A. Devi, A. Kumar, T. Abdeljawad, and A. Khan. Existence and stability analysis of solutions for fractional langevin equation with nonlocal integral and anti-periodic-type boundary conditions. *Fractals*, 28(8):2040006, 2020.

[44] A. A. Thirthar, P. Panja, A. Khan, M. A. Alqudah, and T. Abdeljawad. An ecosystem model with memory effect considering global warming phenomena and an exponential fear function. *Fractals*, 31(10):2340162, 2023.

[45] W. B. Rabie, H. M. Ahmed, T. A. Nofal, and S. Alkhatib. Wave solutions for the (3+ 1)-dimensional fractional Boussinesq-KP-type equation using the modified extended direct algebraic method. *AIMS Mathematics*, 9(11):31882–31897, 2024.

[46] N. Elsonbaty, H. Ahmed, N. Badra, W. Rabie, and M. Eslami. Distinct solitary wave solutions for the (3+1)-dimensional integrable pKP–BKP equation using the modified extended direct algebraic technique. *Computational Methods for Differential Equations*, 2025.

[47] F. Sağlam and S. Malik. Various traveling wave solutions for (2+1)-dimensional extended Kadomtsev–Petviashvili equation using a newly created methodology. *Chaos,*

Solitons & Fractals, 186:115318, 2024.

[48] L. Kaur, A. Biswas, A. Arnous, Y. Yildirim, L. Moraru, and M. Jweeg. Shock wave and singular solitary wave perturbation with Gardners equation having dispersion triplet. *Contemporary Mathematics*, pages 3743–3762, 2025.

[49] R. Khalil, M. Al Horani, A. Yousef, and M. Sababheh. A new definition of fractional derivative. *Journal of Computational and Applied Mathematics*, 264:65–70, 2014.

[50] S. Maqsood, R. Thinakaran, H. Khan, and J. Alzabut. A Logistic Growth Epidemiological SEIR Model with Computational and Qualitative Results. *Euro. J. Pure Appl. Math.*, 18(2):5944, 2025.

[51] N. Wan-Arfah, M. Muzaimi, N. N. Naing, V. Subramaniyan, L. S. Wong, and S. Selvaraj. Prognostic factors of first-ever stroke patients in suburban Malaysia by comparing regression models. *Electron. J. General Medicine*, 20(6):em545, 2023.